Development of Thermoplastic Polyurethane-Hexagonal Boron Nitride Composite Foams with Enhanced Effective Thermal Conductivity

Parisa Ghariniyat

A THESIS SUBMITTED TO

THE FACULTY OF GRADUATE STUDIES

IN PARTIAL FULFILLMENT OF THE REQUIREMENTS

FOR THE DEGREE OF

MASTER OF APPLIED SCIENCE

Graduate Program in

MECHANICAL ENGINEERING

York University

Toronto, Ontario

December 2017

Abstract

Advances in the field of microelectronics have contributed to component miniaturization and therefore have augmented the power densities, resulting in thermal management concerns. High power densities generate an excess amount of heat, which leads to increases in device operating temperature, reduced performance and surges in hardware failure. Traditionally, heat sinks have been used to conduct excess amount of generated heat away and keep the component's temperature to below the critical level in order to prevent the device from permanent damage. In particular, they are often sensitive to thermal cracking and are of limited utility in small and thin packages [1]. Due to this challenge, discovering new multifunctional materials with outstanding thermal conductivity is becoming more important.

Thermally conductive polymer composites can be considered as new alternatives to electronic packaging materials, which are usually based on epoxy. Higher thermal conductivity can usually be obtained by adding larger amounts of filler. However, the addition of filler compromises low density, good processibility, flexibility and, in some cases, electrical insulating properties of polymer-based materials. Therefore, it is important to find a way to achieve high thermal conductivity by adding less filler. In this context, this thesis research aims to develop new, conformable thermally conductive polymer composites. Thermoplastic polyurethane (TPU)-hexagonal boron nitride (hBN) composites fabricated by batch foaming were studied as a case example. In particular, foaming has been proposed in this thesis as a potential route to induce filler alignment along the cell wall, and thereby to establish a thermally conductive network in the material system. However, there is a critical level of cell expansion to perfectly align the fillers around the expanded cells. Further expansion would break the thermally conductive network and decrease TPU foam's thermal conductivity (k_{eff}). Therefore, an understanding of foam morphology

is critical to the rational design of improved thermally conductive TPU foams. First of all, a comprehensive experimental study was conducted to identify the foaming behaviors of TPU foams in order to identify appropriate processing windows that would offer flexibility to develop multifunctional TPU composite and nanocomposite foams. TPU foams were fabricated by batch foaming and characterized. The effect of the foaming process (i.e. saturation temperature and saturation pressure) on pore structure (i.e. cell size and cell population density) was investigated. The results of this research demonstrated that by CO_2 foaming it was possible to produce TPU foams at relatively low temperatures (60°C). The results indicated that the cell size and cell density range are significantly wider at lower saturation pressures to varying foaming temperatures. While TPU foams usually yield extremely high cell population density and small cell size, by applying the appropriate foaming conditions, we prepared foams with a wide range of cell sizes, from 21 to 170 μm, and cell population density from 105 to 108 pore/cm^3. Secondly, these conditions have been used to investigate the foaming-assisted filler alignment in TPU composite and nanocomposite foams for tailoring the thermal conductivity. Foamed samples at lower saturation temperatures (i.e. 20 and 40°C) yielded higher thermal conductivity than solid counterparts.

Lifelong gratitude to my family,

and my late grandma Kokab.

Acknowledgements

First and foremost, I would like to express my special appreciation and thanks to my principal supervisor, Prof. Siu N. (Sunny) Leung, whose knowledge, energy and enthusiasm were critical to this effort. I would like to thank him for tirelessly encouraging, guiding and supporting my research and for allowing me to grow as a research scientist. I sincerely appreciate all his invaluable contributions of time, ideas and funding to make my Master's experience productive and stimulating. I believe that I am tremendously fortunate to have worked with the outstanding truly humble and deeply knowledgeable scholar.

I would like to express my gratitude to the members of the M3lab group. I would like to thank the friendly administrative staff members of the school of Lassond who have been kind enough to advise and help me in their respective roles.

My time at York University was made enjoyable in large part due to the many gorgeous Iranian friends that became a part of my life. I wish to express my sincere love and appreciation to my friends Mehdi Agheli Nejad, Laaya Mahini, Pardis Ghahramani and Amin Shams Khoorami. My sincere thanks also go to my best friends, Mahdieh and Shabnam, who have made all the difference in my life.

Lastly, I wish to express my sincerest love, thanks and deep appreciation to my family for their unconditional love and support. My mom and dad, Fereshteh and Aliakbar, have played an important role in the development of my identity and shaping the individual that I am today. They always believed in me and inspired me to follow my dreams. For his continuous encouragement and support, my husband, Amir, receives my everlasting thanks. He pushed me to study for a Master's degree here and without his help and sacrifice, I could not have completed this thesis. I

am indebted to my lovely brother, Armin, for his practical support in all those things of life beyond doing a Master's degree. Also to my gorgeous sisters and brother, Azadeh, Zari and Arash, who are my dearest friends. They are my life.

Table of Contents

List of Tables

List of Figures

List of Illustrations

A	=	Area
ABS	=	Poly(acrylonitrile-butadiene-styrene) copolymer
AC	=	Alternating current
AIN	=	Aluminum nitride
Al_2O_3	=	Alumina
BeO	=	Beryllium oxide
BN	=	Boron nitride
CBA	=	Chemical blowing agent
cBN	=	Cubic boron nitride
CCC	=	Carbon/carbon composites
CFC	=	Chlorofluorocarbons
CMC	=	Ceramic-matrix composites
CNF	=	Carbon nanofiber
CNT	=	Carbon nanotube
CO_2	=	Carbon dioxide
CTE	=	Coefficient of thermal expansion
DC	=	Direct current
DSC	=	Differential scanning calorimetry
EVA	=	Poly(ethylene vinyl acetate)
GNP	=	Graphene nanoplatelet
hBN	=	Hexagonal boron nitride

HCFC	=	Hydrofluorocarbons
HDPE	=	High density polyethylene
HS	=	Hard segment
k	=	Thermal conductivity
$k_{\parallel}$	=	In-plane thermal conductivity
$k_{\perp}$	=	Through-plane thermal conductivity
k_{eff}	=	Effective thermal conductivity
LCP	=	Liquid crystal polymer
LDPE	=	Low density polyethylene
M	=	Magnification factor
m_{air}	=	Sample's weight in air
MMC	=	Metal-matrix composites
m_{water}	=	Sample's weight in water
n	=	Number of cells
N_0	=	Cell population density
PA6	=	Nylon-6
PA66	=	Nylon-6.6
PBA	=	Physical blowing agent
PBT	=	Poly(butylene terephthalate)
PC	=	Polycarbonate
PDMS	=	Poly(dimethylsiloxane)
PEEK	=	Polyetheretherketone
PEI	=	Polyetherimide

PET	=	Poly(ethylene terephthalate)
PI	=	Polyimide
PMC	=	Polymer-matrix composites
PMMA	=	Polymethylmethacrylate
PP	=	Polypropylene
PPS	=	Polyphenylene sulfide
PPSU	=	Polyphenylsulfone
PS	=	Polystyrene
PSU	=	Polysulfone
PTFE	=	Polytetrafluoroethylene
PU	=	Polyurethane
PVC	=	Polyvinyl chloride
PVDF	=	Polyvinylidene difluoride
RFID	=	Radio-frequency identification
SEM	=	Scanning electron microscopy
SiC	=	Silicon carbide
SiCnp	=	Silicon carbide particles
SS	=	Soft segment
SWCNT	=	Single-wall carbon nanotube
T_g	=	Glass transition temperature
T_m	=	Melting temperature
$T_{m\text{-}high}$	=	Melting point at higher temperature
$T_{m\text{-}low}$	=	Melting point at lower temperature

TPE	=	Thermoplastic elastomers
TPU	=	Thermoplastic polyurethane
vol. %	=	Volume percent
WAXD	=	Wide-angle X-ray diffraction
wt. %	=	Weight percent
ZnO	=	Zinc oxide
ΔH_{fusion}	=	Heat of fusion
ρ	=	Density of a sample
ρ_f	=	Foam density
ρ_s	=	Solid density
ρ_{water}	=	Density of water
ϕ	=	Volume expansion ratio
1D	=	One-dimensional
2D	=	Two-dimensional
3D	=	Three-dimensional

Chapter 1

1.1 Introduction

There has been a long-standing interest in discovering new multifunctional materials with outstanding thermal conductivity and electrical insulation for electronic packaging. Metals with high ordered arrangements of crystals have high thermal conductivity. The major drawback of this type of material is that it is both heavy and expensive. Moreover, it has low electrical resistivity. Among ceramics, some materials possess high thermal conductivity and transfer heat very well (e.g. aluminum nitride), while others possess low thermal conductivity and transfer less heat (e.g. zirconia). One of the main disadvantages of ceramics is that they cannot be shaped easily.

Polymers have been widely used due to properties that have made them attractive for different applications, namely being inexpensive to manufacture, corrosive resistant and lightweight. However, their low thermal conductivity, poor mechanical properties and low electrical conductivity have remained substantial challenges in emerging sectors such as electronics, energy and aerospace. In most applications, some of the polymer properties should be fixed. For example, for heat sink applications, polymer composites have to have high thermally conductivity but low electrical conductivity, whereas, for energy-harvesting applications, thermoelectric nanocomposites need to have high electrical conductivity and low thermal conductivity. In the context of heat management applications, there has been a long-standing interest in tailoring polymers' thermal conductivity by adding nanofillers with high thermal conductivity to polymer matrices such as metal [2], ceramic [3] and carbon-based fillers [4]. An abrupt increase in thermal conductivity is commonly reached by high filler loadings (>30 vol.%) [5] which can also lead to

negative effects on cost, weight and processability of polymer composites. Hence, it is really important to find the most efficient formulation and processing condition to obtain a better thermal conductivity performance without sacrificing other properties. Forming multiple conductive paths in the direction of heat transfer while also providing a very high packing fraction of filler in polymer matrix is one of the most important factors for achieving maximum conductive networks and higher thermal conductivity. This phenomenon can be promoted by different methods, including novel fabrication processes, using hybrid fillers, and using fillers with higher aspect ratios. The alignment of filler particles (typically 1- or 2-directional (1D, 2D)) with high in-plane thermal conductivity can be a good solution to improve thermally-conductive networks and to take full advantage of high in-plane thermal conductivity. Recently, many studies have been conducted to develop fabrication processes which induce filler alignment [6]. As a lower cost can be achieved by reducing the amount of the material, reducing weight is a potential way to make cheaper products. A novel approach to reduce weight and increase the filler alignment in polymers is to produce polymeric foams. Foams have been typically used in applications such as insulation, cushioning or packaging [7]. However, adding high thermally conductive fillers leads to enhanced thermal conductivity. Therefore, incorporating foaming process and functional fillers can be a potential route to develop novel, lightweight polymer composites with outstanding performance. Adding filler increases the rigidity of material while foaming helps to increase the flexibility. Therefore, we can also reduce the cost of material and promote flexibility by foaming.

Thermoplastic elastomers (TPE) is a class of polymers which have both thermoplastic and elastomeric properties. While thermosets involve chemical cross-linking, thermoplastics contain purely physical crosslinks. Therefore, thermoplastics are readily processed (e.g. injection molding and extrusion). This results in lower energy costs for processing and considerably shorter cycle

times. Moreover, TPEs are recyclable and can be easily reprocessed. One of the most commonly used TPEs is thermoplastic polyurethane (TPU). TPUs are unique polymeric materials exhibiting a wide range of physical and chemical properties. They are a commercially important class of thermoplastics that can be tailored to meet the manufacturing challenges in a fast-changing world. TPUs are linear, block copolymers consisting of hard and soft segments. TPUs' multifunctional properties can be tailored by incorporating various types of filler into a TPU matrix while maintaining its uniquely high compliance. Therefore, many studies have been conducted to develop TPU composites. Improved mechanical, thermal and adhesive properties by incorporating nanosilica have been reported [8]. Mishra *et al.* [9] were able to enhance the storage modulus of the dual modified Laponite-TPU nanocomposite in a glassy state (at –60 °C) and in a rubbery state (+98 °C), by172.8% and 85%, respectively. Most of the research on TPU composites has focused on using carbon nanotubes as conductive filler [10]. In addition to TPU composites and nanocomposites, many studies on TPU foams have been reported. Nemat *et al*. [11] studied microcellular TPU foams by using butane as the blowing agent. It was shown that the plasticizing effect of butane induced a wide range of HS crystalline domains. As a result, the presence of HS crystalline domain enhanced cell nucleation with a limited range of cell size (2.5-40μm) and cell density (10^8-10^{11} cells/cm^3) over a wide range of saturation temperatures, from 150°C to 170°C at a saturation pressure of 55 bar. Michaeli *et al.* [12] examined only the correlations between the process parameters and CO_2 solubility in the polymer. It was observed the solubility limit decreased with increasing screw speed for all screw geometries. However, only limited research has been conducted to develop conformable multifunctional TPU composite foams by taking advantage of foaming-assisted filler alignment in TPU matrices. With the continuous development of flexible and wearable electronics, multifunctional materials with good conformability represent

an emerging family of engineering materials in different economic sectors. In this context, this research aimed to investigate the foaming behaviors of TPU foams in order to identify appropriate processing windows that would offer flexibility for researchers to develop multifunctional TPU composite and nanocomposite foams.

1.2 Objective of Thesis

Thermally conductive polymer composites can be new promising for electronic packaging. The higher thermal conductivity can usually be obtained by adding high volume loadings of filler. However, the addition of filler compromises the low density, good processibility, flexibility and, in some cases, electrical insulating properties of polymer-based materials. Therefore, it is very important to find a way to achieve high thermal conductivity by adding less filler.

In this context, this thesis research aims to develop new, conformable thermally conductive polymer composites. Thermoplastic polyurethane (TPU)-hexagonal boron nitride (hBN) composites foamed by batch foaming were studied as a case example. This research was divided into two phases.

1.2.1 Phase One

In particular, foaming is proposed in this thesis as a potential route to induce filler alignment along the cell wall, thereby establishing a thermally conductive network in the material system. However, there is a critical level of cell expansion to perfectly align the fillers around the expanded cells and further expansion would break the thermally conductive network and decrease TPU foam's thermal conductivity (k_{eff}). Therefore, an understanding of foam morphology is critical to the rational design of improved thermally conductive TPU foams. First, a comprehensive experimental study was conducted to identify the foaming behaviors of TPU foams in order to identify appropriate processing windows that would offer flexibility to develop multifunctional

TPU composite and nanocomposite foams. TPU foams were fabricated by batch foaming and characterized. The effect of the foaming process (i.e. saturation temperature and saturation pressure) on pore structure (i.e. cell size and cell population density) was investigated. The results of this research demonstrated that by CO_2 foaming it was possible to produce TPU foams at relatively low temperatures (60°C). The results indicated that the cell size and cell density ranges are significantly wider at lower saturation pressures to varying foaming temperatures. This is because there is a difference in crystallization behaviors of TPU at different saturation pressures. At lower saturation pressure, specifically, there are fewer crystals which can act as heterogeneous nucleating sites. While TPU foams usually yield extremely high cell population density and small cell sizes, by applying the appropriate foaming conditions, we prepared foams with the wider range of cell sizes from 21 to 170 μm and cell population density from 10^5 to 10^8 pore/cm^3.

1.2.2 Phase Two

In the second phase, these conditions were used to investigate the foaming-assisted filler alignment in TPU composites and nanocomposite foams for tailoring their effective thermal conductivity. hBN crystals are anisotropic as a result of their layered structures. Consequently, they have anisotropy in thermal conductivity. The in-plane (in direction within plane) thermal conductivity is reported to be about 300 W/mK [62]. Therefore, aligning the hBN platelet using foaming could be a promising way to take advantage of high in-plane thermal conductivity. Polymer nanocomposite foams were fabricated with batch foaming using CO_2 as a physical foaming agent. Nanocomposite samples were first heated in a stainless-steel chamber to a temperature around the melting point of the polymer matrix. The compressed CO_2 was then released and pressurized into the chamber for a given time to saturate the specimens. Subsequently, rapid depressurization of chamber caused thermodynamic instability of super-saturated specimens.

This provided the driving force for nucleation and growth of CO_2 bubbles within the polymer matrix. The cell structure of foamed samples was stabilized through a cooling process close to room temperature. By injecting CO_2 into the composite melt in the foaming process, the expansion of cells would align the hBN platelets along the cell walls. Consequently, better thermally conductive networks would be developed in the TPU matrix, thereby enhancing the k_{eff} and overcoming the thermal insulation property of polymer foams.

1.3 Thesis Structure

This thesis is organized into six chapters.

Chapter one provides an introduction to polymer composite and foaming-assisted filler alignment. The objectives of the thesis are described.

Chapter two presents a literature review and background information of related previous research. The various methods of changing the intrinsic thermal conductivity of polymers are discussed.

Chapter three demonstrates the materials and processing methods which have been used to fabricate TPU foams.

Chapter four demonstrates the effect of the foaming process (i.e. saturation temperature and saturation pressure) in a pore structure (i.e. cell size and cell population density).

Chapter five presents the foaming-assisted filler alignment in TPU composite and nanocomposite foams for tailoring the thermal conductivity.

Chapter six summarizes the major contributions and conclusions. It also provides recommendations or avenues for future research.

Chapter 2
Literature Review

2.1 Flexible and Wearable Electronics

One of the most active and vibrant new fields today is developing flexible and wearable electronics due to the emergence of next-generation portable electronic devices, such as the portable display, computing, communication and identification products. Wearable electronics are electronic devices which can be worn by a person either internally (i.e. implants) or externally (i.e. accessories) [13]. The internal electronic device can be a pacemaker while externally it can be a monitoring ring or a sensor. Most wearable devices are uncomfortable to wear due to their rigidity and weight. As a result, the essential factors that should be considered for the design of multifunctional wearable electronics are that they be lightweight, durable, energy-efficient, comfortable and robust. Wearable electronics operate as a sensor or as a computer. Consequently, the materials used in designing wearable electronics should be flexible, lightweight and conductive. Fiber-based clothing is the preferred candidate as the platform for wearable electronics because they are flexible, washable and durable [14]. The convergence of the positive features of textiles technologies, electrical engineering and electronic components is a potential way to combine the speed of growing modern electronics, with the flexible, wearable and continuous nature of fiber-based materials [15] . Many wearable electronic textiles consist of different layers which are in contact either with skin or electronic parts.

In recent decades, the idea of adding fibers or fiber assemblies (textile structures) to electronics has been of great interest. Fiber-based flexible electronics have garnered much attention in a wide range of applications such as conformable circuits [16], interfacing computers/processors [17], pressure sensors [18], flexible radio-frequency identification (RFID) [19], and other emerging

applications [20-23]. Wearable electronics also have a great potential for use in certain types of garments such as for military, healthcare and personal electronics. The health monitoring system is one such feasible application [21]. Wearable biosensor systems for health monitoring have received extensive attention from academic and industrial researchers during the last decades [22,23]. Various types of miniature sensors, wearable or even implantable, have been used in wearable health monitoring systems.

For wearable electronics, the choice of materials to fabricate a sustainable flexible system which confer high flexibility and good electrical performance, is the most important consideration. Most available commercially conductive yarns are made up of polymer composites. Polymers are intrinsically insulators, therefore a potential way to make them conductive is to add highly conductive fillers such as carbon black, carbon nanofibres, metal particles and ceramics. However, adding a high volume fraction of filler to polymers would compromise their flexibility. Accordingly, there are still challenges to fabricate a flexible polymer composite with high thermal or electrical conductivity.

2.2 Electronic Packaging

Increasing electronic packaging density and reliability have resulted in a need for new multifunctional material to meet all the requirements. In order to reduce any thermal stresses, packaging material should have a tailorable coefficient of thermal expansion (CTE) which could be matched to substrate materials. The CTEs of semiconductors like silicon and gallium arsenide are in the range of about 4-7 PPM/K [24]. Therefore, the CTE of the material used for substrates should be in the same range in order to minimize thermal stresses in packaging [25]. However, the CTE of materials with good thermal conductivity, such as aluminum and copper, are much higher than desired.

Advances in the field of microelectronics have contributed to component miniaturization and therefore augment the power densities, resulting in thermal management concerns in electronic packaging design. As the reliability of a transistor depends on the operating temperature, and as a microprocessor operates at a greater speed, it is vital to keep the operating temperature low. On the other hand, the continuing increase in electronic packaging density has resulted in a need for new, advanced material with high thermal conductivity, low cost, low weight and a tailored CTE [26]. Low cost and low density are also key considerations. In this context, the plastic packaging has become popular. However, their low moisture resistance is a major drawback. As conventional packaging materials do not meet all criteria, developing new composite materials has been attracting great interest [24,27]. Combining different components is a potential way to fabricate new advanced composites with great advantages for thermal management in electronic packaging. Composite materials are defined in four classes: polymer-matrix composites (PMCs), metal-matrix composites (MMCs), ceramic-matrix composites (CMCs) and carbon/carbon composites (CCCs) [28]. Aluminum matrix and copper matrix composites are common MMCs used for electronic packaging. Their CTE can be typically tailored by introducing a reinforcing agent such as carbon fiber, silicon carbide (SiC) and diamonds [29,30]. However, all MMCs are electrically conductive, which is not favorable in many applications.

At this time, in the interests of low cost, a low dielectric constant and ease of processing, polymer composites play an important role in electronic packaging. Polymer properties can be easily tailored by blending with different types of fillers. Polymer-matrix composites provide unique combinations of properties which make them outstanding candidates for electronic packaging. In today's microelectronic packaging industry, the leading packaging material is epoxy

composites for device encapsulation due to their low cost and high reliability. Traditionally, epoxy composites have been used in electronic packaging for device encapsulation [31-33].

2.3 Thermally Conductive Polymeric Material Systems

2.3.1 Pure Polymer

Over the last 50 years, the usage of polymers has grown enormously. With the continuous technological advances in the electronic industry, the power density, and thereby the amount of heat generation of components, has surged dramatically in recent decades. Indeed, the

Table 2.1. Thermal Conductivities of Some Polymers [34,35]

Material	Thermal Conductivity at 25 °C (W/m K)
Low density polyethylene (LDPE)	0.30
High density polyethylene (HDPE)	0.44
Polypropylene (PP)	0.11
Polystyrene (PS)	0.14
Polymethylmethacrylate (PMMA)	0.21
Nylon-6 (PA6)	0.25
Nylon-6.6 (PA66)	0.26
Poly(ethylene terephthalate) (PET)	0.15
Poly(butylene terephthalate) (PBT)	0.29
Polycarbonate (PC)	0.20
Poly(acrylonitrile-butadiene-styrene) copolymer (ABS)	0.33
Polyetheretherketone (PEEK)	0.25
Polyphenylene sulfide (PPS)	0.30
Polysulfone (PSU)	0.22
Polyphenylsulfone (PPSU)	0.35
Polyvinyl chloride (PVC)	0.19
Polyvinylidene difluoride (PVDF)	0.19
Polytetrafluoroethylene (PTFE)	0.27
Poly(ethylene vinyl acetate) (EVA)	0.34
Polyimide, Thermoplastic (PI)	0.11
Poly(dimethylsiloxane) (PDMS)	0.25
Epoxy resin	0.19
Thermoplastic polyurethane (TPU)	0.28

inability to sufficiently dissipate heat from the devices has imposed another limitation in many new devices. In this context, new materials that can contribute to thermal management of these components are of interest to the electronics industry. While high cost heat sinks have traditionally been used to promote heat dissipation, the industry is demanding new thermally conductive materials that can be integrated with the electronic packaging in order to streamline the production process as well as to reduce manufacturing costs and the components' sizes. In this context, polymeric material systems represent an important material family due to properties that make them attractive for heat transfer applications, namely being inexpensive to manufacture, corrosive-resistant and lightweight. Yet their low thermal conductivity is the main challenge. The thermal conductivity of common polymers is listed in Table 2.1.

In recent years, changing the intrinsic thermal conductivity of polymers has been an active area of research [36-38] . Choy *et al.* introduced this idea early, in 1970 [38]. While polymers are generally insulators because of entanglement of the molecular chains, Choy *et al.* [37,38] demonstrated that mechanical stretching increases the chain alignment, so heat can flow more efficiently down the polymer chains (the chain axis). This plays an important role in increasing the intrinsic thermal conductivity of polymers. The experimental data show that thermal conductivity of crystalline regions is at least an order of magnitude larger in the chain axis direction $k_{||}$ than in perpendicular $k_{\perp}$[39]. By stretching these polymers, a higher degree of chain alignment is achieved. This increases the thermal conductivity parallel to the stretching direction and decreases it in the perpendicular directions. In the perpendicular direction, thermal conductivity decreases due to less-oriented chain axes in those directions. However, an economical high-volume manufacturing process which will enable a polymer system to form either heat exchanger or heat

sink is still missing. It remains unknown how much improvement can be achieved by stretching polymers [35].

2.3.2 Polymer Composites

Thermal management has a fundamental role in the packaging industry, especially in electronic devices. It is certainly crucial to adequately dissipate heat to increase the performance and reliability of electronic devices. Polymeric materials with high thermal conductivity have received more attention in thermal management systems. Therefore, metals and ceramics parts can be replaced by polymers in heat transfer devices and systems, which result in energy and cost savings. Furthermore, polymers can be readily converted to polymer composites in different forms (e.g. bulk and coating forms) because of their low processing temperatures.

Table 2.2. Thermal Conductivities of Common Thermally Conductive Fillers [40]

Material	Thermal Conductivity at 25 °C (W/m K)
Aluminum	234
Nickel	91
Gold	315
Copper	400
Lead	30
Iron	84-90
Aluminum Oxide	38-42
Boron Nitride	29-300
Silicon Carbide	85
CNT (single wall)	≈6000
CNT (multi wall)	≈3000
Carbon fiber	260

The thermal conductivity of polymers can also be enhanced by adding fillers with high thermal conductivity to polymer matrices such as metal [41], ceramic [3] and carbon-based fillers [4]. Fillers also can be classified based on their structures as one-dimensional (1D), two-dimensional

(2D), and three-dimensional (3D). For instance, single-walled carbon nanotubes (SWNTs) are one-dimensional (1D) fillers. Boron nitride (hBN) and graphene are two-dimensional (2D). Common three-dimensional (3D) fillers include carbon black and cubic boron nitride (cBN).

In order to achieve maximum thermal conductivity, filler selection is crucial. The capability of fillers to form multiple heat flow paths which also give a very high packing fraction act as important factors in improving the thermal conductivity network. Some studies have also proved filler effectiveness with large particle sizes, various particle distribution models and low aspect ratios for obtaining better packing [42]. Fillers with perfect crystal structures can decrease phonon scattering, which results in increased thermal conductivity. In Table 2.2, the thermal conductivities of common thermally conductive fillers are listed [43].

Many studies on polymeric composites with different base materials and fillers have been reported [44]. However, different composites cannot be compared directly, because each group of researchers has applied different manufacturing procedures. Also, due to such differences in the same type of fillers as their crystal structure, size and shape, it might be meaningless to compare the same materials, bases and fillers. Adding filler also leads to poor mechanical properties (i.e. fragility). Further, using fillers increases the cost of final material. Therefore, great care should be taken to ensure good thermal conductivity, mechanical properties, stability and low cost. It is really difficult to tailor a composite with these desired properties.

Typically, effective thermal conductivity (k_{eff}) of polymer composites depends on the three main factors: structure and properties of polymer and fillers; alignment and orientation of the filler inside the polymer, and the interactions between the filler surface and the polymer matrix. The thermal conductivity of polymer composites is strongly affected by the filler type, loading level, filler size, and filler shape. Moreover, the spatial alignment and orientation of the filler are also

important to consider effective thermal conductivity. Fillers can be aligned during processing. Therefore, we can get full advantage of anisotropic thermal conductivity in the composite. For example, some plate-like fillers (e.g. hBN) have high k_{eff} in plane, so if they can be perfectly oriented, the k_{eff} in plane would strongly affect the k_{eff} of the polymer composite. Many novel techniques are being developed in order to obtain the desired filler orientation.

One of the keys to achieving high thermal conductivity in the composite is creating a filler network. However, this is usually formed at high filler loading levels which can result in high costs, poor processability and poor mechanical properties. Much research is in progress to develop composites with high thermal conductivity at a lower filler loading level.

Filler-polymer compatibility is also important. Poor interaction between the filler and polymer matrix surface can result in high thermal interfacial resistance and can decrease thermal conductivity. Therefore, improving polymer-filler interfacial interaction can considerably increase the thermal conductivity of composites. [45].

2.3.2.1 Type of Fillers

2.3.2.1.1 Metal Fillers

Polymer composites filled with metal have attracted the attention of many engineering fields. This is due to the fact that adding metallic particles to a polymer matrix increases electrical conductivity of the composites while keeping the processing condition and mechanical properties the same as the polymers [46]. However, there are few publications on the study of thermal conductivity of such composites [47] . Aluminum and copper are commonly used as thermal conductive fillers in polymer-metal composites. Bigg [48] showed that if the difference between thermal conductivity of the filler and the polymer matrix is greater than 100-fold, it has no significant effect on the thermal conductivity of the composite. As a result, polymers cannot take

full advantage of fillers with high thermal conductivity, such as metals. Furthermore, metals are both thermally and electrically conductive while most ceramic materials are an electrical insulator. Hence, appropriate ceramic materials can be used in applications where both thermal conductivity and electrical insulation are required.

2.3.2.1.2 Carbon-based Fillers

Carbon-based fillers (e.g. carbon nanotubes and carbon fibers) provide many potential applications because they have a higher thermal conductivity, excellent corrosive resistance and a lower thermal expansion coefficient than metals. Carbon-carbon composite is the system in which the matrix and filler are both carbon materials. This carbon-carbon composite has very high thermal conductivity and is the most suitable material system to form a heat sink. But they are very expensive, so mass production of this system for industrial purposes faces many challenges. For this reason, development of cheap polymer composites filled with carbon-based fillers has been studied by different research groups. Some common thermal conductive carbon-based fillers are graphite, carbon fiber, diamonds and carbon nanotube. The development of nanocomposites based on carbon nanofiber (CNF) and carbon nanotube (CNT) has been intensively studied, in which CNF and CNT have been used as fillers to make use of their physical properties. These fillers can improve not only mechanical properties but also electrical and thermal conductivity. For example, CNTs have been used to improve mechanical properties of polymers [49-52], since they are much stronger. But weak nanotube/matrix bonding causes difficulties in improving mechanical properties of the composites. On the other hand, CNTs have recently been embedded into polymers to create materials with better electrical and thermal transport properties [53,54]. CNT and CNF are the most promising candidate materials for thermally-conductive composites because of their high thermal conductivity. By using some important models for predicting thermal conductivity

of composites, CNT and CNF -filled nanocomposites show higher thermal conductivity enhancement than any other inorganic fillers. In reality, however, the thermal conductivities of composites are relatively low. This is due to the large interfacial thermal resistance between the CNT and the polymer matrix which prevents the transfer of phonons (which control heat conduction) in polymers [4]. As mentioned earlier, if the difference between thermal conductivity of the filler and the polymer matrix is greater than 100-fold [48], the filler has no significant effect on the thermal conductivity. Therefore, carbon-based fillers are not good candidates for polymers. Haggenmueller *et al.* [51] also showed that embedding a single-wall carbon nanotube (SWCNT) does not have a significant effect on thermal conductivity of composites.

2.3.2.1.3 Ceramic Fillers

Polymer composites have been used for device encapsulation in electronic packaging. Actually, encapsulation of electronic devices increases their long-term reliability and protects them from an unfavorable environment. Traditionally, epoxy/silica composites have been widely used for encapsulation. However, due to low thermal conductivity (1.5 W/mK) of silica [3], these composites show a very poor thermal performance. As aforementioned, higher thermal conductivity can be achieved by using thermally conductive fillers. However, polymers cannot take full advantage of high thermal conductive fillers such as metals and carbon-based fillers.

Ceramic fillers are the preferred material to improve the thermal conductivity of polymers such as hexagonal boron nitride (hBN), aluminum nitride (AIN) and silicon carbide (SiC). In addition, ceramics are widely used as fillers because of their high thermal conductivity and electrical resistivity [52,55].

Table 2.3. Comparison of BN with Other Thermally Conductive Fillers [54]

	BN	AIN	Al_2O_3	SiO_2	ZnO
Thermal properties					
Thermal conductivity (W/mK)	300	260	30	1.4	54
Specific heat (J/Kg.K, 25°C)	794	734	798	689	523
Theoretical density (g/cc)	2.25	3.26	3.98	2.20	5.64
Electrical properties					
Dielectric constant	3.9	8.8	9.7	3.8	9.8
Volume resistivity	1015	1014	1014	1014	107
Mechanical properties					
Thermal expansion coefficient (ppm/K)	<1.0	4.4	6.0	0.5	0.7
Youngs Modulus (GPa)	40	400	340	72	12
Knoop Hardness (kg/mm^2)	11	1200	1500	500	387

However, the thermal conductivity of silica is too low, 1.5 $W \cdot m^{-1} \cdot K^{-1}$, so the effective thermal conductivity of silica-filled polymer composites is limited. Therefore, researchers have sought to increase thermal conductivity with higher thermally conductive ceramic fillers such as beryllium oxide (BeO), hexagonal boron nitride (hBN) [10], aluminum nitride (AlN) [53], alumina (Al_2O_3) [56] and zinc oxide (ZnO) [57]. However, extreme hardness of AIN is its major disadvantage as there are many difficulties in processing and limitations in the application of an AlN/polymer composite [58]. Aluminum oxide (Al_2O_3) and zinc oxide (ZnO) have a relatively high thermal conductivity and are widely used as fillers due to their low cost and high electrical resistivity. But they have high dielectric constants and cannot be used for insulation applications [59]. Moreover, most of these filler materials, except boron nitride as shown in Table 2.3, are hard and abrasive and this can cause severe damage to the equipment during processing. In contrast, hBN is much softer with very high intrinsic thermal conductivity; hence it is preferred over other ceramic fillers. In addition, soft hBN particles can easily be deformed so can give better packing density to form

thermally conductive networks [60]. Large particle size grades of such fillers also reduce surface areas, which lead to decreased interfacial phonon scattering. Furthermore, larger particles reduce filler-polymer interfaces which result in decreasing the number of thermally resistant junctions [61].

Several extensive studies have been conducted regarding outperforming hBN in improving the thermal conductivity of polymer composites [62-67]. Tsutsumi *et al.* [68] studied a polyimide system filled with diamond, alumina, aluminum nitride, boron nitride and silicon carbide. It was observed that by 54 vol% hBN loading, a maximum value for thermal diffusivity with a ten-fold increase compared to the neat polymer can be achieved.

2.3.2.2 Formation of thermally Conductive Networks

Forming multiple conductive paths in the direction of heat transfer while giving a very high packing fraction, is the most important factor in achieving maximum conductive networks and higher thermal conductivity. This phenomenon can be promoted by different methods: specific fabrication process; using hybrid fillers, and using fillers with a higher aspect ratio.

The alignment of filler particles can be a good solution to improve the thermal conductivity. Many studies have been conducted to develop a fabrication process which induces filler alignment. Different methods have been reported, such as electric field-induced filler alignment [6,69], magnetic field-induced filler alignment [70], ultra-drawing [59], ultra-sonication [50], and foaming [53]. Park *et al.* [69] studied aligned single-wall carbon nanotube ("SWCNT") polymer composites by using an electric field. The observed orientation of field-induced SWCNT networks offered the potential route to produce composites with the required properties for a specific application by easily tuning the applied field strength, frequency, and time. Martin

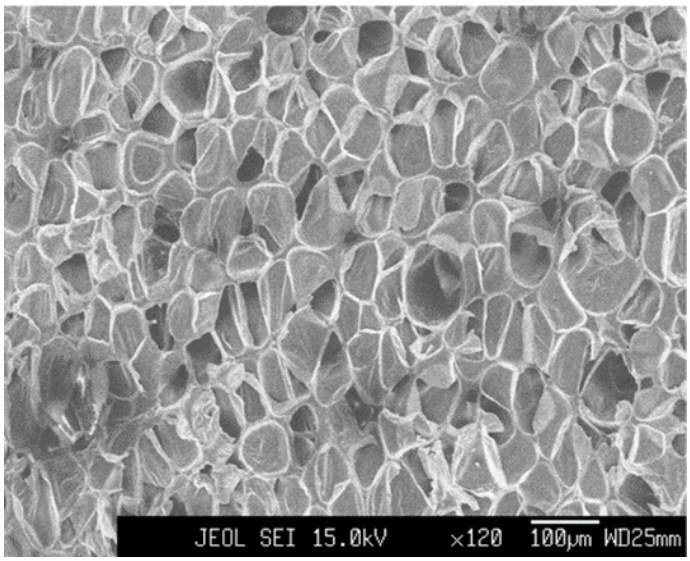

Figure 2.1. Biaxial-flow Alignment of Clay Particles Along the Cell Boundary in a Polypropylene Matrix During Foaming Processing [53]

et al. [6] also studied electric field-induced filler alignment to create aligned conductive CNT networks in epoxy-based composites. It was demonstrated that a CNT can be aligned by both AC and DC electric fields. However, networks formed in AC fields are more uniform and more aligned compared to DC fields. In the study of using a magnetic field to align multi-wall carbon nanotubes (MWCNT) in a polyester-based composite, Kimura *et al.* [70] showed that MWCNT-polymer composite has better percolation path for the parallel direction than perpendicularly. This anisotropic nature of such a filler provides a novel method to prepare specific composites with anisotropic properties. Leung *et al.* [59] revealed that alignment of liquid crystal polymer (LCP) fibrils could be enhanced by ultra-drawing of LCP- graphene nanoplatelet (GNP) composite which led to increasing the thermal conductivity of the composite. Yu *et al.* [71] dispersed hybrid GNP-SWNT fillers in the epoxy-based polymer by using ultra-sonication which led to achieving a composite with thermal conductivity of 3.35 $W \cdot m^{-1} \cdot K^{-1}$ with only 20 wt% of filler. Recently, many studies have been conducted on the application of foaming to induce filler alignment in a polymer matrix [53,72]. Ding *et al.* [72] showed that foaming has the potential to assist filler alignment and

filler network which enhance the thermal conductivity of polymer material systems. Further, Okamoto *el al.* [53] investigated the biaxial-flow alignment of clay particles along the cell walls in a polypropylene matrix during foaming processing.

A hybrid filler composed of two or more fillers showed that the combination offered the novel ability to improve composite performance by taking advantage of each filler [3,56]. This hybrid filler system helps to create massive thermally conductive networks by bridging the fillers. It also helps to greatly decrease the overall filler loading, hence reducing the system's viscosity [57]. In the study of thermoplastic polyurethane filled MWCNT/graphene hybrid filler, Roy *et al.* [10] showed that by adding 0.25 and 0.50 wt.% MWCNT–CRGO to TPU thermal stability and storage modulus improved significantly due to uniform dispersion of fillers in the polymer matrix and strong interfacial interaction between TPU and the filler. Yu *et al.* [71] studied the effect of a nanoscale hybrid filler composed of SWCNT and graphite nanoplatelets (GNP). It was demonstrated that it significantly improved thermal conductivity of epoxy-based composites, which is attributed to the formation of a more efficient thermal conductivity network with significantly reduced thermal interface resistance. Geon *et al.* [3] investigated the hybrid filler comprising different fillers like aluminum nitride (AlN), wollastonite, silicon carbide whisker (SiC) and boron nitride (BN). It was found that hybrid fillers can be an effective way to increase the thermal conductivity of the composite. This is probably due to the more efficient connectivity which is offered by structuring a filler with a high aspect ratio in the hybrid filler. Teng *et al.* [73] studied the thermal conductivity of epoxy-based composites filled with two hybrid fillers, MWCNTs and AlN, in which a small amount of functionalized MWCNT (1 vol.%) in an AlN/epoxy composite with 25 vol.% modified AlN loading showed comparable thermal conductivity (1.21 W/mK) to that of epoxy composite containing 50 vol.% untreated AlN (1.25

W/mK), which can reduce by half the amount of AlN filler used. Furthermore, Lee *et al.* [4] showed that the effect of hybrid fillers (AlN/wollastonite) is more than that of a single-size filler in enhancing thermal conductivity of the composite.

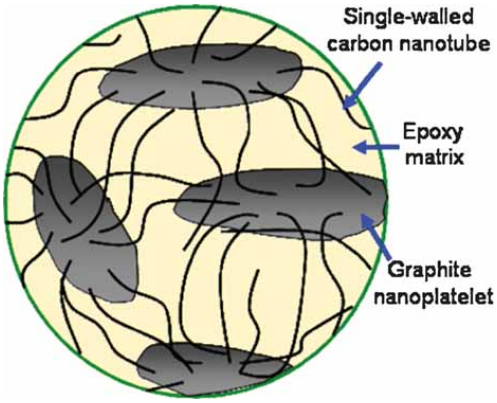

Figure 2.2. Schematic of GNP-SWCNT Network in Polymer Matrix [71]

The aspect ratio can have a significant effect on the thermal conductivity of composites [74]. Kochetov [75] investigated the effect of the size and shape of the filler on the thermal conductivity of epoxy-based composites. Large particle size grades of fillers reduce the surface area, which leads to a decrease in interfacial phonon scattering. As a result, composites filled large particle size grades of fillers show higher thermal conductivity.

2.3.2.3 Particle Surface Modification

The surface modification of the particles has been employed by a number of researchers in order to decrease the filler-matrix thermal contact resistance which led to achieving higher thermal conductivity [76,77]. Surface treatment of the filler minimizes the interfacial phonon scattering. Phonons can scatter through several mechanisms as they travel through the material such as phonon-phonon scattering, phonon-impurity scattering, phonon-electron scattering, and phonon-boundary scattering. This helps to improve the wettability and uniform dispersion of the filler in the polymer matrix. As a result, effective thermal conductivity will increase. For example, Xu and

Chung [58] investigated the effect of surface treatment of BN with different materials (e.g. acetone, silane, HNO_3 and H_2SO) in epoxy-based composites. It was clearly shown that the surface treatment of the particles resulted in an increase of thermal conductivity of BN and AlN particle epoxy-based composites by up to 97%. This is due to an improvement of the interface between the matrix and particles which leads to decreasing interfacial resistance between the fillers and the matrix.

Yang and Gu [60] studied the effect of surface treatment of the hybrid filler MWCNTs/ nano-sized silicon carbide particles (SiCnp) on the thermal conductivity of epoxy nanocomposites. It was shown that the thermal conductivities epoxy composites filled with silane-modified SiCnp were larger than those of epoxy composites filled unmodified SiCnp. It could be due to making the connection between SiCnp to the epoxy matrix and reducing the resistance to the heat flow caused by epoxy–SiCnp interface. Improved thermal conductivity was achieved by such surface treatment. It could be ascribed to the fact that TETA functionalization improved the interfacial heat transport between the epoxy matrix and the MWCNTs and helped to create better dispersion of MWCNTs in the matrix, which is beneficial to the improvement of the thermal conductivity of MWCNT/epoxy composites.

2.3.3 Polymer Composite Foams

Over recent decades, the foaming process to produce microcellular polymer has been extensively investigated. Due to the versatile nature of polymeric-based foams, they have been used for various applications including packaging materials, sound insulation, thermal insulation, shock absorption, cushioning, and bioscaffolds for tissue engineering [78,79]. The reason polymer foams are so widely used is that they have numerous advantages, such as low density, good thermal insulation, and superior toughness.

There are various methods for fabricating porous polymer composites including batch foaming, extrusion foaming, and foaming with expancel® microspheres. The foaming process typically includes several steps: dissolution of a blowing agent (PBA or CBA) into a polymer matrix under an elevated pressure; generation of pores or cells upon inducing thermodynamic instability (i.e. rapid depressurizing to the ambient pressure); the growth of nucleated bubbles in the polymer, and finally, stabilization of the porous or cellular structure.

2.3.3.1 Blowing Agent

The blowing agent is the dominant factor in both the manufacturing and performance of polymer foam. The blowing agent can be either a physical blowing agent (PBA) or a chemical blowing agent (CBA). In the PBA process, the gases (i.e. volatile liquids or compressed gases) are injected directly into the polymer system. Park has extensively studied this method, (Mucell® process) [80][81]. Several types of PBAs have been used, such as chlorofluorocarbons (CFCs), CO_2 and N_2. However, PBA foaming needs special equipment such as a gas injector, a high-pressure gas source and a specially designed chamber or screw. Despite the technical challenges, PBAs are still common blowing agents in industries due to their lower cost and effectiveness, especially in the production of low-density foams. CFCs were traditionally used as blowing agents, but as they deplete the ozone layer and negatively affect global warming [82] they are being phased out as blowing agents in the foam industry. Hydrofluorocarbons (HCFCs) and perfluorocarbons (PFCs) are also to become subject to strict environmental regulations and are to become restricted compounds. They can be replaced with alternative candidates, such as HFCs, nitrogen, hydrocarbons and carbon dioxide, all of which have low environmental effects, nonflammability and low toxicity [83]. Inert gases, especially CO_2 and N_2, are generating much interest since they are environmentally friendly and do not deplete the ozone layer [86]. In the supercritical state,

materials become dense like a liquid but maintain a gas-like ability to flow with almost no viscosity or surface tension. As a result, their solubility in a polymer increases significantly due to which the glass transition temperature (Tg) of most polymers reduces. The solubility of CO_2 in most common polymers is much higher than that of N_2 and other inert gases. CO_2 is used extensively to make thermoplastic foams such as PU foams. Therefore, CO_2 will be used in this study to make TPU foams due to higher solubility and good plasticization effects.

Chemical blowing agents (CBA) are compounds that release the gas either due to thermal decomposition or due to chemical reaction [84]. N_2 or CO_2 are typical gases which are produced by CBAs' decomposition [85,86]. CBA reactions can be categorized into two groups: endothermic or exothermic. Azodicarbonamide (ACD) is the world's most commonly-used exothermic CBA which generates N_2 upon decomposition, with decomposition temperatures between 170°C and 200°C. Sodium bicarbonate and zinc bicarbonate are the best representative endothermic blowing agents. The main advantage of CBAs is the ease of process. However, the bubbles obtained with CBAs are larger than those obtained with PBAs and this results in lower mechanical properties.

2.3.3.2 Batch Foaming

The basic solid-stage batch foaming is a two-stage process which is shown schematically in Figure 2.3. In the first stage, the polymer is placed in a high-pressure chamber. This step is usually conducted at an ambient temperature. Over a given time, the gas diffuses into the polymer matrix to saturate the sample. Subsequently, rapid depressurization of the chamber causes thermodynamic instability of super-saturated specimens. In the second stage, the supersaturated specimen is immersed in a heated bath with a temperature above the glass transition temperature (T_g) of the polymer-gas mixture for a given time. Nucleation and growth of the bubbles within the polymer matrix happen during this stage. The sample is then cooled to stabilize the foam structure

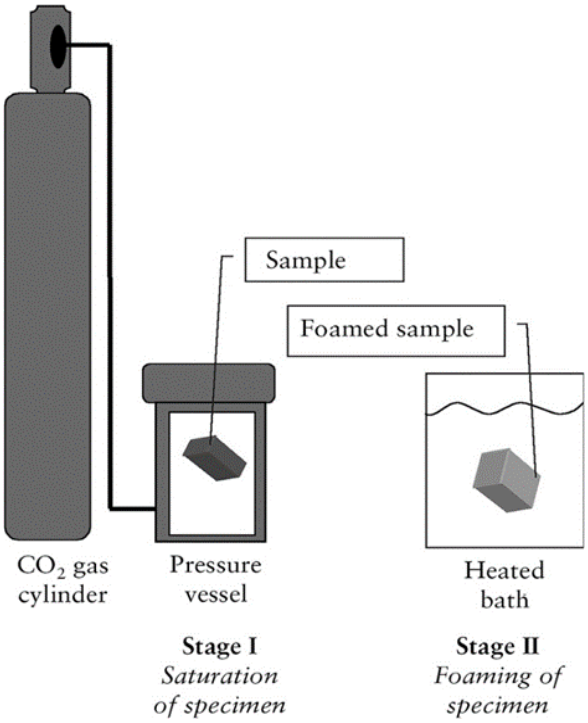

Figure 2.3. Schematic of The Solid-State Batch Process [87]

The main disadvantage of solid-state batch foaming is the low diffusivity rate of blowing the agent into the polymer matrix at an ambient temperature. Accordingly, there is another type of batch foaming which is conducted at an elevated temperature (i.e. higher than T_g and lower than T_m of the polymer), termed the foaming temperature. Batch foaming is used in this study due to its simple operation and easy control of experimental parameters to produce foams with tailored properties.

2.3.3.3 Extrusion Foaming

In extrusion foaming processes, polymers and additives are first melted and mixed in a heated barrel with a rotating screw. Subsequently, the blowing agent is injected to the plastic melt via decomposition of CBA or direct injection of PBA. Screw designs with good mixing and energy transfer capability have been developed to achieve a homogeneous plastic-gas mixture with uniform temperature, additive and blowing agent distribution. These mixing techniques enhance

the homogeneity of the polymer-additive-gas mixture and its temperature distribution, which is crucial for foaming. A series of division and deformation of plastic melt to disperse local gas pockets are applied to achieve the final mixture. In this process, the energy and mass transport are accelerated due to an increased polymer-gas interface area and decreased striation thickness. Subsequently, the uniform polymer-gas mixture is forced through a die and foaming is induced by a rapid depressurization upon the mixture exiting the die. The sample is cooled under ambient conditions or immersion in water to stabilize the foam structure.

2.3.3.4 Foaming with Expancel® Microspheres

Expancel® microspheres are polymeric microspheres which consist of a polymer shell encapsulating a gas. They expand when heated within a specific temperature range. The microsized bubbles consist of a polymer shell encapsulating a hydrocarbon gas. When heated, the internal pressure of the gas inside the sphere increases and the thermoplastic outer shell softens, resulting in a significant increase in the volume of the microspheres. The gas remains inside the spheres. Researchers have investigated using expandable polymeric microspheres as a blowing agent to create porous materials. They have also studied the effect of temperature on the morphology of the foams [88,90]. This is a novel processing route for foaming and as such it has been considered non-conventional. It was observed that there is an optimal processing temperature to obtain the lowest density for composites formed with Expancel® microspheres, which is variously based on the grade of microsphere used. Below this optimal temperature, the viscosity of the polymer is too high, hence bubble growth is limited. Above this temperature, due to a high rate of diffusivity, gas loss is unavoidable [89]. Therefore, the processing temperature is the dominant factor to find a balance between gas loss and expansion rate resistance for Expancel® microspheres. In the study

of closed-cell ceramic foams fabricated using Expancel® Microspheres, Kim *et al.* [91] used various microsphere content and the temperature to tailor the porosity of the material.

2.4 Elastomers

Generally, polymers can be divided into three categories: thermoplastics, thermosets, and elastomers (rubbers). Thermoplastics are polymers that become homogenized liquid above a specific temperature and harden upon cooling. They can be melted and shaped several times due to which property they are called reversible materials. Thermoplastic materials are either crystalline or amorphous. Thermosets are amorphous polymers which only have one chance to liquefy and be shaped when heated. They decompose by further heating and do not reform upon cooling. Elastomers are amorphous polymers existing above their glass transition temperature so are relatively soft and deformable at ambient temperature.

Viscosity plays an important role in choosing a suitable polymer for the matrix. Lower viscosity helps to form a thin layer between thermally conductive filler particles, which leads to reducing thermal resistance. Moreover, it allows a higher concentration of fillers to be incorporated into the system, which results in achieving higher thermal conductivity. However, the wettability and the adhesion between the fillers and polymers also have a great effect on reducing interfacial phonon scattering [3]. The molten thermoplastic polymer has good filler wettability and leads to high bond strength [92].

Thermoplastic polyurethanes (TPUs) are a commercially important class of thermoplastics, exhibiting a wide range of physical and chemical properties. By tailoring their microstructures, it is possible to also tailor their properties to meet manufacturing challenges in a fast-changing world [93] TPUs are linear, block copolymers consisting of alternating sequences of hard and soft segments. This alternating block structure was first suggested by Cooper and Tobolsky [94]. The

soft segment can be either a polyether or polyester type. A polyether-based TPU is generally used in wet environments while a polyester-based TPU suits applications where resistance to oil and hydrocarbons is essential. Depending on the type of isocyanate, the HS (i.e. isocyanates) can be classified as either aliphatic or aromatic. By manipulating the proportion of hard and soft segments, it is possible to produce different degrees of hardness. The flexible amorphous soft domains influence the elastic nature of TPUs while the rigid semi-crystalline hard domains influence elastic modulus, hardness, tear strength and melt processing [95]. For example, a higher hard-to-soft segments ratio will result in a more rigid TPU. Due to the thermodynamic incompatibility between these two segments, phase separation occurs and results in micro-domain structures. There are many factors governing the morphology and final properties of polyurethane (PU) and TPU. These include: state of segregation [93,96], the length of the HS [97-99], thermal history [100] and mechanical history [101,102]. In particular, varying the thermal history can alter TPU's microphase structure [103].

Polyurethane block polymers generally contain a high degree of hydrogen bonds [104]. Various techniques, such as fourier transform infrared spectroscopy (FTIR), differential scanning calorimetry (DSC), wide-angle X-ray diffraction (WAXD) and optical microscopy, were used to study the crystallization behavior and intermolecular bonding of TPU [105-107]. Clough *et al.* [106] investigated the structural organization and transitions in both polyether-based and polyester-based urethane elastomers. The results revealed that there are three characteristic thermal transitions, being the glass transition and two higher transitions due to the disruption of hydrogen bonding. The low temperature peaks (i.e. 70°C – 80°C) were related to the disruption of urethane-macroglycol bonds. The high temperature peaks (i.e. 150°C – 180°C) were due to the disorder of urethane-urethane bonds in HS. The sizes and positions of these endothermic peaks were governed

by many factors, including composition ratio, thermal annealing, thermal history and processing condition [108-110]. Thermal annealing of TPUs would rearrange hydrogen bonds and thereby enhance the formation of HS domains and their crystallization kinetics [111] .

2.4.1 TPU Composites

TPUs' multifunctional properties can be tailored by embedding various types of filler in a TPU matrix while maintaining its uniquely high compliance. In this context, many studies have been conducted to develop TPU composites and nanocomposites. Improved mechanical and adhesive properties by incorporating nanosilica were reported [112]. TPU nanocomposites filled with zinc oxide have been fabricated. Pulsed laser ablation of zinc in a polymer offers a simple synthesis to produce semiconductor ZnO/polymer composites, which are promising materials for biomedical and photovoltaic devices [113]. A lot of work has been done on TPU composites loaded SWCNTs [114] and MWCNTs [115]. However, the use of CNTs has been limited because of the difficulties associated with dispersion of CNT during processing and poor interfacial interaction between CNTs and the polymer matrix. This is due to the small diameter of CNTs in the nanometer scale with high aspect ratio (>1000) which results in an extremely large surface area [116]. Therefore, surfactant and covalent functionalization have been employed to have better dispersion [117-119]. Most of the TPU-CNT nanocomposites have been commonly fabricated by solution processing techniques [120,121]. In situ polymerization [122]and melt mixing [123] have also been reported. Mishra *et al.* [9] found that the fabrication of TPU nanocomposites filled with dual modified synthetic hectorite nanoclay could increase the storage modulus by 172.8% and 85% over neat TPU in the glassy region (i.e. -60°C) and in the rubbery region (i.e. 98°C), respectively. Most of the research of TPU composites has focused on using carbon nanotubes as conductive fillers [120,121,123,124]. Bilotti *et al.* [125] studied the electrical and mechanical properties of TPU

fibers containing MWCNTs. Their nanocomposite fibers were able to achieve an electrical conductivity of ~3 $S \cdot m^{-1}$ with 3 wt.% CNT loading. A recent study demonstrated that an optimal loading of natural fiber (i.e., Kenaf) could significantly reinforce TPU [126]. Moreover, Haung *et al.* [127] fabricated TPU-few-layered graphene nanocomposites with enhanced mechanical properties and extremely high self-healing efficiencies (i.e. > 98%). As aforementioned, carbon-based fillers cannot be used in applications in which electrical insulating is important. As a result, further promoting thermal conductivity of polymer composites by replacing CNTs with the preferred ceramic filler, hBN, can enhance the thermal conductivity of polymer composites (i.e. the incorporation of fillers with higher thermal conductivity with low dielectric constant) while electrical insulating is also favored. Nobody has yet prepared a thermally conductive TPU composite.

2.4.2 TPU Foams

In recent years, TPU foamed products have become more important in industry. They have been used in a variety of applications such as furniture, automobile interiors and sporting applications, including athletic shoes, sports shoes, ski boots and in-line skates, due to their easy processability and desirable, customizable properties. [128]. Moreover, their biocompatibility, high fracture strain, moderate tensile strength and excellent abrasion and tear resistances make them extremely popular for medical applications [129]. Several methods have been used to fabricate TPU foam, such as electrospinning [130], thermal induced phase separation [131], extrusion [12], batch foaming [132] and microcellular injection molding [133]. The last two methods have attracted a great deal of interest due to absence of organic solvents.

The foaming condition to produce microcellular TPU has been extensively investigated. Hossieny *et al.* [11] showed that incorporating butane in TPU improved the crystallization of hard

segments which resulted in enhanced cell nucleation. Nema *et al.* [134] investigated the effect of different blowing agents (i.e. exo- and endothermic) on the morphology of TPU foams. It was found that the exothermic blowing agent (i.e. azodicarbonamide) should be used only with a special commercial additive which could decrease the decomposition temperature of azodicarbonamide. In addition, the density of TPU foams could be reduced up to 40%. A potential way to improve the TPU properties is by introducing fillers to the TPU matrix. Wang *et al.* [135] showed that nanoclay can significantly promote crystal nucleation and cell nucleation. On the other hand, nanoclay plays an important role as an effective nucleation agent. Accordingly, adding nanoclay resulted in a foam structure with a smaller cell size and a higher cell density compared to neat TPU. Moreover, nanoclay also has good reinforcement effects. As a result, the tensile strength was enhanced by 56.3% and 89.2% with 5 and 10 wt% clay contents, respectively. Kharbas *et al.* [133] studied the effect of a cross-linking agent on the foam morphology of TPU fabricated by microcellular injection molding. It was found that incorporating a cross-linking agent in the TPU matrix increased the melt strength. Consequently, lower densities could be achieved by foaming at the higher temperature and greater pressure.

2.5 Summary

Over recent years, the applications of polymers have grown enormously due to properties that have made them attractive for different applications, namely being inexpensive to manufacture, corrosive resistant and lightweight. Yet their low thermal conductivity, poor mechanical properties and electrical conductivity are the main challenges in emerging sectors such as electronics, energy, and aerospace. Therefore, more attention has been given to the idea of tailoring polymers' properties by adding fillers to polymer matrices such as metal [41], ceramic[3], and carbon-based fillers [4]. However, high filler loading can also lead to negative effects on cost, weight, and

processability of polymer composites. As reducing costs can be achieved by reducing the density of the material, foaming has attracted significant attention as a way to decrease the cost and increase the applications of polymers. Therefore, incorporating a foaming process and functional fillers is a potential route to develop novel lightweight polymer composites.

Recently, many studies have been conducted on the applications of foaming to induce filler alignment in a polymer matrix[53,72]. Ding *et al.* [72] showed that foaming has the potential to assist filler alignment and filler network which enhance the thermal conductivity of polymer material systems. In a similar way, Yan *et al.* [136] fabricated electrically-conductive PU foams with a low electrical percolation threshold by only 1.2 wt.% carbon nanotubes loading. This was achieved by controlling the filler dispersion in the cell walls, which resulted in the formation of electrically-conductive pathways. Ling *et al.* [137] have recently fabricated lightweight polyetherimide (PEI) composites for EMI shielding by combining foaming with a small amount of graphene. It was observed that microcellular foaming induced perfect orientation of graphene along the cell walls. This created an effective electrically-conductive graphene path at lower graphene loadings (i.e. 0.18 vol. %).

TPUs are unique polymeric materials exhibiting a wide range of physical and chemical properties. They are a commercially important class of thermoplastics that can be tailored to meet the manufacturing challenges of a fast-changing world [138]. Embedding different types of filler into the TPU matrix can tailor TPU's multifunctional properties while maintaining its uniquely high compliance. Therefore, many studies have been conducted to develop TPU composites. Improved mechanical and adhesive properties by incorporating nanosilica have been reported [139]. While the uses of CNT have been limited because of the difficulties in uniformly dispersing CNT within the TPU matrix, extensive studies have been conducted to study TPU/CNT

nanocomposites. Bilotti *et al.* [125] studied the electrical and mechanical properties of TPU fibers containing MWCNTs. They were able to achieve the electrical conductivity of ~3 S m^{-1} with 3 wt. % of CNT loading.

In addition to TPU composites and nanocomposites, many studies on TPU foams have been reported. Nemat *et al.* [11] studied microcellular TPU foams by using butane as the blowing agent. It was demonstrated that the plasticizing effect of butane induced a wide range of HS crystalline domains. As a result, the presence of hard segments (HS) in the crystalline domain enhanced cell nucleation over a wide range of saturation temperatures ranging from 150°C to 170°C at a saturation pressure of 55 bar. Yeh *et al.* [132] studied four types of polymer foams and revealed that TPU foams were the most promising due to the possibility of achieving extremely high cell population density and small cell size. Moreover, they investigated the effect of nanoclay as a nucleation agent on the TPU foams' morphology.

However, limited research has been conducted to develop conformable multifunctional TPU composite foams by taking advantage of foaming-assisted filler alignment in TPU matrices. With the continuous development of flexible and wearable electronics, multifunctional materials with good conformability represent an emerging family of engineering materials in different economic and industrial sectors. In this context, this research aims to investigate the foaming behaviors of TPU foams in order to identify appropriate processing windows that offer flexibility for researchers to develop multifunctional TPU composite and nanocomposite foams.

Chapter 3
Experimental and Sample Characterization

3.1 Materials

Commercially available TPU (Estane® 2103-70A TPU, Lubrizol) was used as the base polymer. hBN platelets (PolarTherm powder grade AC6041) were purchased from Momentive Performance Materials Inc. Carbon dioxide (CO_2) of 99.8% purity (Linde Gas Inc.) was used as the physical blowing agent for the batch foaming of TPU. The physical properties of TPU and hBN are summarized in Tables 3.1 and 3.2, respectively.

Table 3.1. Physical Properties of TPU

Property	Value	Unit
Density	1060	$kg \cdot m^{-3}$
Melting temperature	171-181	°C
Softening temperature	75	°C
Shore hardness	72	A

Table 3.2. Physical Properties of hBN

Property	Value	Unit
Density	2280	$kg \cdot m^{-3}$
In-plane thermal conductivity ($k_{\parallel}$)	300+	$W \cdot m^{-1} \cdot K^{-1}$
Through-plane thermal conductivity ($k_{\perp}$)	~3	$W \cdot m^{-1} \cdot K^{-1}$
Lateral size	6	μm
Thickness	0.1-0.5	μm
Specific surface area	8	m^2/g

3.2 Sample Preparation

In the first set of experiments of neat polymer, TPU pellets were ground into fine powders by a mill freezer (SPEX SamplePrep Group, model 6770, Freezer/Mill). Particle sizes ranged from 250 μm to 500 μm. The TPU powders were then dried in a vacuum oven at 80°C for 12 hours.

In the second set of experiments of polymer composite, TPU pellets were first dried for at least 4 h at 90 °C in a vacuum oven. Then TPU pellets and hBN (5, 10 and 15 vol. %) powder were melt-mixed at 190 °C for 5 min at 75 rpm using a compounder (HAAKE™ MiniCTW Micro-Conical Twin Screw). The extruded material was cooled in a water bath and cut into small pellets. Prior to compression molding, calculated amounts of TPU-hBN batch were dried again for 4 h at 90 °C in a vacuum oven.

The materials were then compression-molded into circular disc samples of 120 mm in diameter and 500 μm in thickness by the following procedures.

STEP 1. TPU powders were charged into a circular disc mold and loaded into a compression molding machine (Craver Press, 4386 CH) preset at 210°C.

STEP 2. The sample and the mold were equilibrated at the preset temperature for 1 min while contacting the heating platens to completely melt the TPU powders.

STEP 3. The sample and the mold were pressurized gradually to 30 MPa to compression mold the materials into thin-disc samples.

STEP 4. The heaters of the compression molding machine were turned off the samples while the molded sample was solidified under pressure.

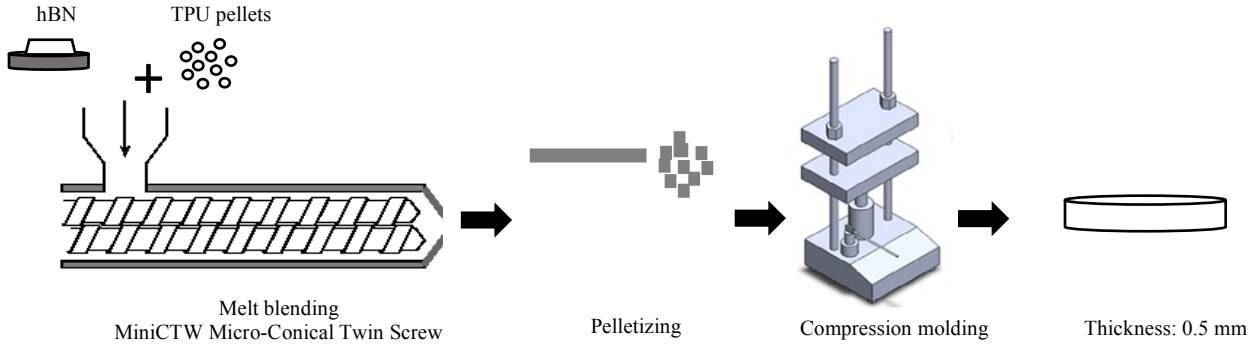

Figure 3.1. Procedures of sample preparation

3.3 Batch Foaming of TPU-hBN Composite Using Supercritical CO_2

The fabrication of TPU foams was performed by carbon dioxide (CO_2) foaming. All samples were pre-cut into square-shaped samples of 2 cm by 2 cm before being foamed. First, the samples were loaded into a high pressure/high temperature vessel. Once the vessel was heated to the preset temperature, it was then saturated with CO_2 at elevated pressure and temperature for one hour. The saturation time had been selected to ensure sufficient time to saturate the TPU with CO_2. After that, the pressure of the vessel was rapidly decreased by releasing the CO_2 from the vessel. This would lead to thermodynamic instability in the saturated sample. The cell structure of foamed TPU was stabilized by submerging it in an ice bath. The schematic of experimental setup is shown in Figure 3.2. The key parameters used in the foaming experiments are summarized in Table 3.3.

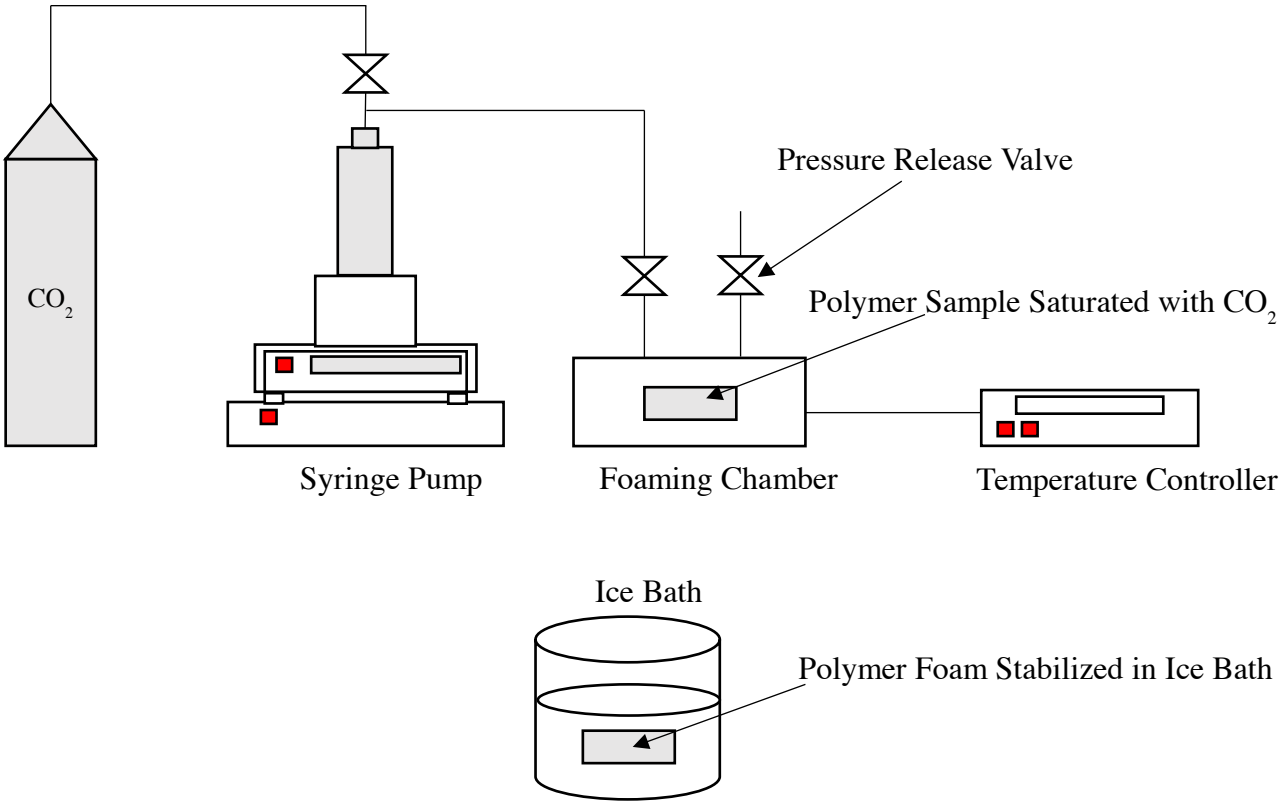

Figure 3.2. Schematic of The Experimental Setup

Table 3.3. Parameters in Foaming Experiments

Variable	Value	Unit
Saturation Pressure	1200, 1600, 2000	psi
Saturation Time	1	hr
Foaming Temp.	20, 40, 60, 80, 100, 120	°C

3.4 Sample Characterization

The apparent density of TPU foam samples were determined in accordance to ASTM D792. After measuring their weights in air and in water, the apparent density (ρ) and the volume expansion ratio (∅) can be determined by Equations (1) and (2), respectively.

$$\rho = \frac{m_{air}.\rho_{water}}{m_{air} - m_{water}} \quad (1)$$

where ρ is the apparent density of a sample, m_{air} and m_{water} are the sample's weights measured in air and water, respectively, and ρ_{water} is the density of water.

$$\emptyset = \frac{\rho_s}{\rho_f} \quad (2)$$

where ρ_s and ρ_f are the densities of solid and the foam samples.

The foam morphology of TPU-hBN foams was characterized by scanning electron microscopy (FEI Company Quanta 3D FEG). The cross-sections of all samples were exposed by cryofracturing the samples in liquid nitrogen. The fractured surfaces were sputter-coated with gold (Denton Vacuum, Desk V Sputter Coater). The cell size and cell population density were obtained by analyzing the SEM micrographs of the foams. The cell population density (N_0) with respect to the unfoamed volume was determined by Equation (3).

$$N_{\circ} = \left[\frac{nM^2}{A}\right] \times \emptyset \quad (3)$$

where n is the number of cells in the SEM micrograph, M is the magnification factor, and A is the area of the micrograph.

The effective thermal conductivity (k_{eff}) of TPU-hBN composite and its foams was measured with a thermal conductivity analyzer (C-Therm Technologies Ltd., Tci Thermal Conductivity Analyzer).

Chapter 4

CO_2 Foaming of Thermoplastic Polyurethane: From Crystallization to Foam Morphology

4.1 Introduction

Thermoplastic polyurethanes (TPUs) are unique polymeric materials with a wide range of physical and chemical properties [138]. This versatile polymer can be used in different applications either as a soft engineering plastic or as a replacement for hard rubber. TPU is well-known for such outstanding properties as high elongation and tensile strength, elasticity and, to varying degrees, its ability to resist oil, grease, solvents, chemicals and abrasion. These characteristics make TPU extremely popular across a range of applications including automotive instrument panels, caster wheels, power tools, sporting goods, medical devices, drive belts, footwear, inflatable rafts, and a variety of extruded film, sheet and profile applications. TPUs are linear, block copolymers consisting of alternating sequences of hard and soft segments. The soft segment can either be a polyether or polyester type, depending on the application. For example, a polyether-based TPU is generally used in wet environments while oil and hydrocarbon resistance require a polyester-based TPU. The hard segments are isocyanates and can be classified as either aliphatic or aromatic depending on the type of isocyanate. For even greater utility, the proportion of hard and soft segments can be manipulated to produce a wide range of hardness. The flexible amorphous soft domains influence the elastic nature of TPU while the rigid semi-crystalline hard domains influence elastic modulus, hardness, tear strength and melt processing [95]. Therefore, a greater ratio of hard to soft segments will result in a more rigid TPU.

One of the interesting research areas of TPU is in the fabrication of its foams. Nemat *et al.* [11] successfully produced microcellular TPU foams by using butane as the blowing agent. It was

shown that the plasticizing effect of butane induced a wide range of HS crystalline domains. These HS crystalline domains enhanced heterogeneous cell nucleation and resulted in foams with small cell size (2.5 – 40μm) and high cell density (10^8 – 10^{11} cells/cm^3) over a wide range of foaming conditions. Michaeli *et al.* [12] examined the correlations between the processing parameters and CO_2 solubility in TPU. It was observed that increasing the screw speed during foam extrusion would reduce the solubility of CO_2 in TPU. Yeh *et al.* [132] studied four types of polymer foams and found that TPU foams was the most promising type due to the possibility of achieving extremely high cell population density and small cell size. Moreover, they confirmed the presence of nanoclay would positively influence the TPU foams' morphology. With continuous development of flexible and wearable electronics, multifunctional materials with good conformability represent an emerging family of engineering materials in different economic sectors.

Various studies have also focused on the application of foaming to induce filler alignment in the polymer matrix [53][72][140]. Ding *et al.* [72] demonstrated that foaming-assisted filler alignment and networking enhance the thermal conductivity of polymer-hexagonal boron nitride material systems. Similarly, Yan *et al.* [141] fabricated electrically conductive PU foams with a low electrical percolation threshold (i.e., only 1.2 wt.% CNT loading). This was attributed to the enhancement of establishing electrically conductive pathways due to the localization and alignment of CNT along the cell walls. Ling *et al.* [137] recently fabricated lightweight polyetherimide (PEI) nanocomposite foams with enhanced EMI shielding performance. It was also observed that microcellular foaming assisted the alignment of graphene along the cell walls. This facilitated the formation of electrically conductive graphene networks at very low graphene loadings (i.e., 0.18 vol. %). Okamoto *et al.* [53] showed that foaming-induced biaxial flow would

enhance clay particles' alignment along the cell boundary in a polypropylene matrix. Moreover, the reinforced cell walls would suppress cell rupture. Nam *et al.* [140] also produced polypropylene-clay nanocomposite foams via batch foaming with clay particles aligned along the cell walls.

The aim of this work is to investigate the effects of CO_2 foaming conditions on the crystalline structures and the foam morphologies of TPU. It also aims to elucidate the interrelationship between TPU crystallization and foaming. While TPU foams generally yield extremely high cell population density and small cell sizes, it is important to identify processing conditions that can yield a wide range of cell morphologies. The outcomes can provide insights for researchers and manufacturers to tailor TPU's foam structure to meet different needs. In the long run, the concepts can be extended to fabricate multifunctional TPU composite and nanocomposite foams with enhanced properties.

4.2 Results and Discussion

4.2.1 Effect of CO_2 on Crystallization Behaviors of TPU

Figure 4.1 shows the DSC thermograms of the compression-molded TPU sample and those saturated with CO_2 at 100°C and different saturation pressures (i.e. 1200 psi to 2000 psi) but without foaming. Table 4.1 summarizes the characteristic properties of the melting peaks in all samples. All samples showed broad melting peaks, which suggested the existence of polydisperse HS crystalline structures in them. The melting temperatures of crystallites formed by the HS chains depend on their degrees of perfection. The crystallites with lower degrees of perfection melt at a lower temperature (i.e., $T_{m\text{-}low}$) while those with higher degrees of perfection melt at a higher temperature (i.e., $T_{m\text{-}high}$). As indicated in Figure 4.1, the TPU samples saturated with CO_2 showed lower onset temperatures (i.e. T_{onset} ~116°C to 118°C) in their melting peaks and larger total areas

under the melting peaks than the compression molded TPU sample without undergoing CO_2 saturation. This trend was more pronounced as the saturation pressure increased from 1200 psi to 2000 psi. Moreover, after annealing the TPU under CO_2, double melting peaks, with $T_{m\text{-}low}$ at around 127°C to 129°C and $T_{m\text{-}high}$ at around 159°C, were observed in the DSC endotherms. Such double peaks were absent in the endotherms of the compression molded TPU without undergoing annealing. Although saturating TPU by CO_2 did not deviate its $T_{m\text{-}high}$, it must be noted that higher saturation pressures resulted in a more prominent melting peak at $T_{m\text{-}high}$.

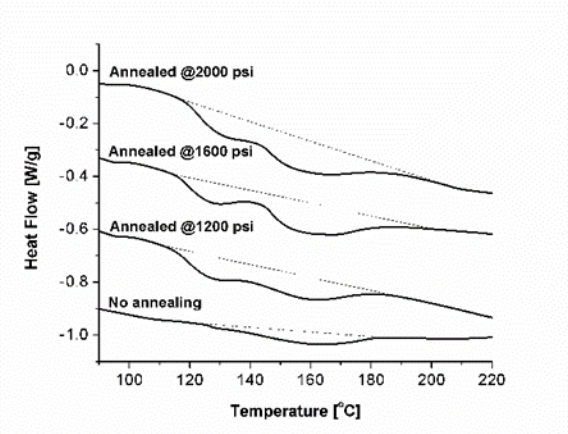

Figure 4.1. DSC Thermogram of a Compression-Molded TPU Sample

Table 4.1. Effects of Annealing under CO_2 (at 100°C) on TPU's Thermal Properties

Saturation Pressure (psi)	ΔH_{fusion} (J/g)	$T_{m\text{-}onset}$ (°C)	$T_{m\text{-}low}$ (°C)	$T_{m\text{-}high}$ (°C)
w/o annealing	3.6	123.7	-	159.1
1200	4.2	115.8	126.6	159.6
1600	5.2	116.2	127.0	159.2
2000	5.4	118.3	129.3	158.8

For TPU samples saturated with CO_2, the plasticizing effect promoted molecular chain mobility, and thereby enhanced HS flexibility. This would facilitate the formation of loosely packed crystallites in regions where crystallite structures were absent before the saturation of CO_2.

The presence of these low perfection crystallites was evidenced by the presence of a new melting peak at the lower temperature range (i.e., $T_{m\text{-}low}$) as well as an increase in the area under the lower temperature range of the broad melting peaks. Moreover, the more identifiable melting peaks at high temperatures in the endotherms of the annealed TPU samples could be attributed to the presence of high perfection crystallites. The increases in the amounts of these high perfection crystallites were also facilitated by the CO_2 enhanced HS chain mobility.

The onset of the broad melting peak of the annealed TPU sample, regardless of the saturation pressure, was at approximately 116°C - 118°C. With the presence of CO_2 during foaming, the initial CO_2 saturation stage served as an annealing step that would influence the crystallization behaviors of TPU. Furthermore, the broad melting peaks would also shift to lower temperatures due to the plasticizing effect of CO_2 [142]. The degree of peak shifting would be more pronounced at higher saturation pressure. Furthermore, the broad melting peaks spanned over the range of foaming temperatures being investigated in this study. Therefore, it was anticipated that the CO_2-influenced TPU crystal structures would affect the foaming behaviors and thereby the foam morphology of TPU. It would in turn affect the potential processing windows to manufacture TPU foams with specific morphology. Furthermore, researchers have investigated how foaming-assisted filler alignment and networking would enhance the multifunctional properties, such as electrical conductivity [141][137] and thermal conductivity [72], of polymer composites and nanocomposites. The elucidation of the processing-to-structure properties of TPU foams would also provide critical information to fabricate TPU composite and nanocomposite foams with the appropriate foam morphology to tailor the filler networking within polymer matrices.

4.2.2 Effects of Processing Conditions on TPU Foams' Volume Expansion

Parametric studies were conducted to investigate the effect of saturation pressure (i.e. 1200, 1600, and 2000 psi) and that of foaming temperature (i.e. 40, 60, 80, 100, and 120°C) on the volume expansion of TPU foams. Figures 4.2(a) through (c) show the changes in the volume expansion ratios of TPU foams over time after the batch foaming process. Regardless of the saturation pressure, TPU foams prepared at 100°C or below shrank dramatically over the first hour and changed only negligibly thereafter, following the physical foaming process. In contrast, the volume expansion ratios of TPU foams prepared at 120°C were virtually unchanged over time. Moreover, lower foaming temperatures resulted in more prominent foam's volume reduction over time. The reduction in TPU foam's volume expansion ratio over time could be attributed to the elastic recovery, which is due to the physical cross-links among the rigid segments and presence of the flexible segments in the thermoplastic elastomer. At lower foaming temperatures (i.e. 100°C or below), the TPU molecular chains had limited mobility, leading to a higher degree of volume recovery after foam expansion. At the higher foaming temperature (i.e. 120°C) together with the plasticizing effect of CO_2, there was improved mobility of molecular chains around expanding cells. This in turn resulted in a more dimensionally stable foam structure.

The volume expansion ratios of TPU foams prepared under different processing conditions were measured after leaving them under ambient conditions for 24 hours and are plotted in Figure 4.3. Regardless of the saturation pressure, the typical mound-shaped curves were observed [53]. As the temperature increased from 40°C to 100°C, the elevated temperature caused a higher degree of crystal melting. As a result, the thermal energy promoted the flexibility of the soft segment (SS), and thereby enhanced the expansion of TPU. However, when the foaming temperature further increased to 120°C, the excessive loss of a blowing agent at an elevated temperature contributed

to the decrease in TPU foam's volume expansion ratio. This observation is consistent with the typical observation in extrusion foaming of thermoplastic [142].

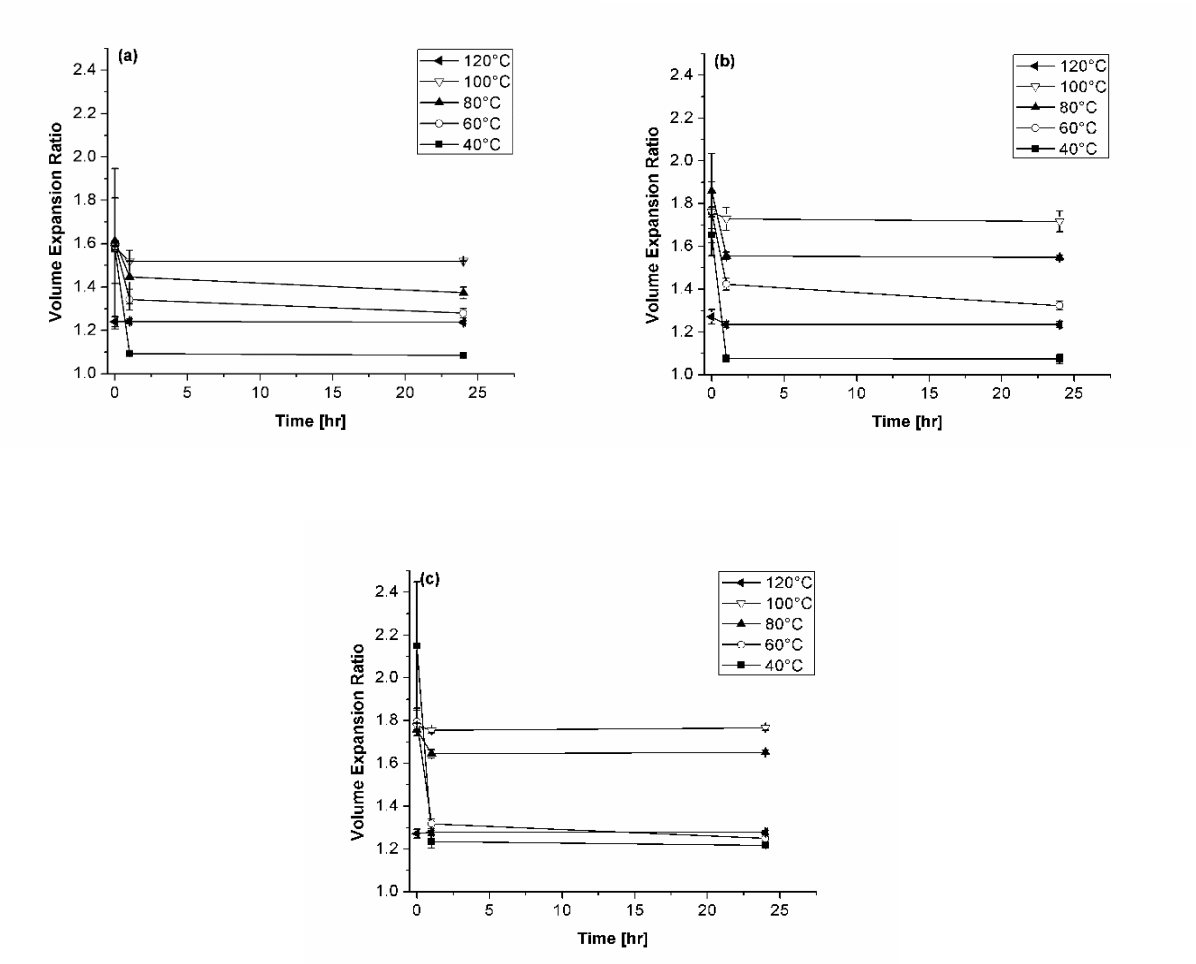

Figure 4.2. Changes in TPU Foam's Volume Expansion Ratio over Time under Ambient Conditions (Saturation Pressure: (a) 1200 psi; (b) 1600 psi; and (c) 2000 psi)

4.2.3 Effects of Processing Conditions on TPU Foams' Morphology

In order to elucidate the effects of processing conditions on TPU's foaming behaviors, the foam morphologies of TPU foams were analyzed using SEM. Figures 4.4 - 4.6 illustrate the SEM micrographs of the cryo-fractured cross-sections of TPU foams fabricated at different combinations of saturation pressure and temperature. It can be observed that the processing window to fabricate uniform TPU foams was wide. In general, a higher saturation pressure, which

helped to dissolve a larger amount of CO_2 in the TPU matrix, resulted in a higher degree of thermodynamic instability during the rapid depressurization process. Therefore, a higher cell population density and more uniform cell morphology were achieved as the saturation pressure increased from 1200 psi to 2000 psi. Increasing the foaming temperature also showed positive effects on promoting cell population density and cell size uniformity. This could be attributed to the increase of TPU molecular chain mobility and suppression of elastic recovery after foam expansion. However, when foaming temperature was higher than an optimal level, cell coalescence (e.g. Figure 4.4(e)) or cell collapse (e.g. Figure 4.5(e)) started to occur. These negatively affected the cell morphology of the TPU foams. The aforementioned gradual temperature dependence of TPU's foam morphology was evidenced in the SEM micrographs of all TPU foams, except that there was an abrupt morphological change in foams fabricated at a saturation pressure of 1200 psi when the foaming temperature increased to 100°C or higher.

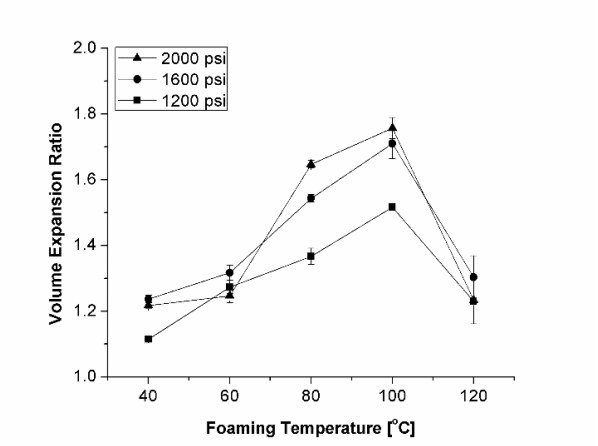

Figure 4.3. Effect of Foaming Temperature and Pressure on TPU Foam's Volume Expansion

In particular, Figures 4.4(c) - (e) reveal TPU foams prepared at 1200 psi had their average cell size increase significantly from around 40 μm, by more than 400%, to over 160 μm. The cell population density also exhibited a dramatic decrease. These observed changes in cell population density and cell sizes suggest that a significantly reduced cell nucleating power occurred when the

foaming temperature changed from 80°C to 100° and above for TPU foams fabricated at a saturation pressure of 1200 psi. Cell nucleation during polymeric foaming requires CO_2 molecules to form nuclei that can overcome a free energy barrier in order to expand spontaneously. Such a free energy barrier is lower if a bubble nucleates heterogeneously (i.e. on the surface of a second phase such as additives or discontinuous phases) instead of homogeneously (i.e. in the bulk phase of the TPU-CO_2 mixture). In addition, the generation of local stress during bubble expansion in proximity of an additive particle or at the boundary of discontinuous phases [143] would also increase the degree of supersaturation and thereby enhance cell nucleation. In this context, the presence of crystalline structures in TPU matrices would promote cell nucleation through the same mechanism. The anticipated evolution of the HS crystalline phases during the CO_2 saturation stage at an elevated temperature would significantly influence the TPU's foam morphology.

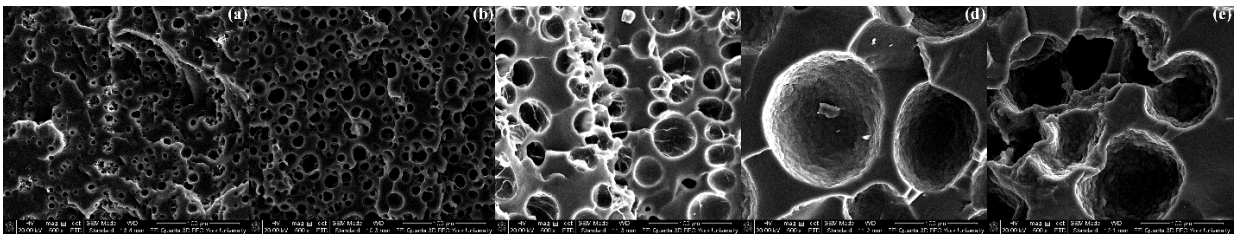

Figure 4.4. SEM Micrographs of TPU Foams Prepared at 1200 psi and Different Foaming Temperatures: (a) 40°C; (b) 60°C; (c) 80°C; (d) 100°C; and (e) 120°C

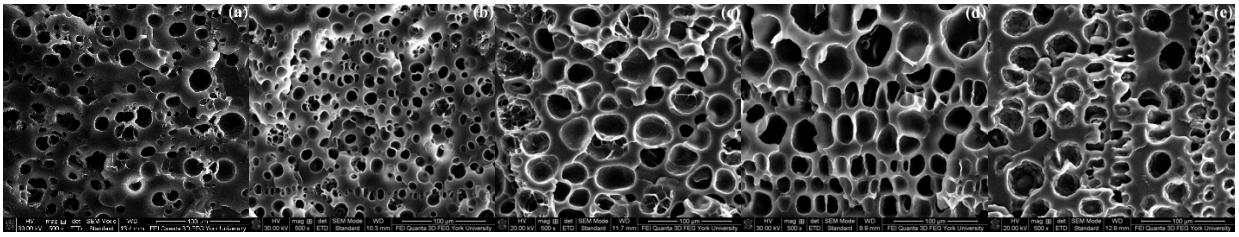

Figure 4.5. SEM Micrographs of TPU Foams Prepared at 1600 psi and Different Foaming Temperatures: (a) 40°C; (b) 60°C; (c) 80°C; (d) 100°C; and (e) 120°C

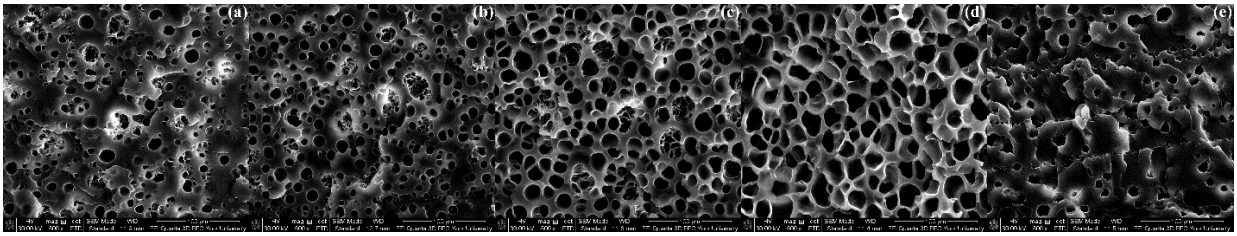

Figure 4.6. SEM Micrographs of TPU Foams Prepared at 2000 psi and Different Foaming Temperatures: (a) 40°C; (b) 60°C; (c) 80°C; (d) 100°C; and (e) 120°C

Figures 4.7 and 4.8 plot the cell population density with respect to the unfoamed volume and the average cell size, respectively, of the TPU foams fabricated at different foaming temperatures and saturation pressures. As expected, TPU foams prepared at higher saturation pressures resulted in more but smaller cells. This was caused by the surged nucleating power with increased CO_2 content within the polymer matrix.

Experimental results revealed that cell population density increased when the foaming temperature slightly increased from 40°C to 60°C, but it decreased when the foaming temperature continued to increase. However, the sensitivity of the cell population density on varying foaming temperatures was more pronounced when the TPU foamed at a lower saturation pressure, especially at 1200 psi. In contrast, the average cell size increased with foaming temperatures from 40°C to 100°C at all saturation pressures, with the effect being more dramatic again for the foams prepared at 1200 psi. When the foaming temperature further increased to 120°C, the average cell size decreased. As the foaming temperature increased, the increase in CO_2 diffusivity would promote the cell expansion. However, as the temperature continued to increase, the excessive gas loss to the surrounding environment would eventually lead to smaller cell sizes.

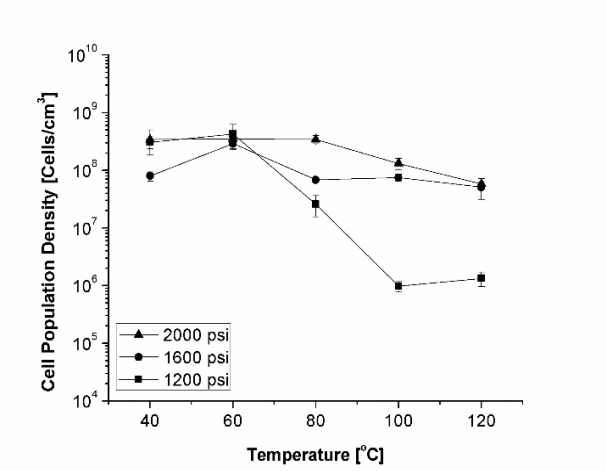

Figure 4.7. Effect of Foaming Temperature and Pressure on TPU Foam's Cell Population Density

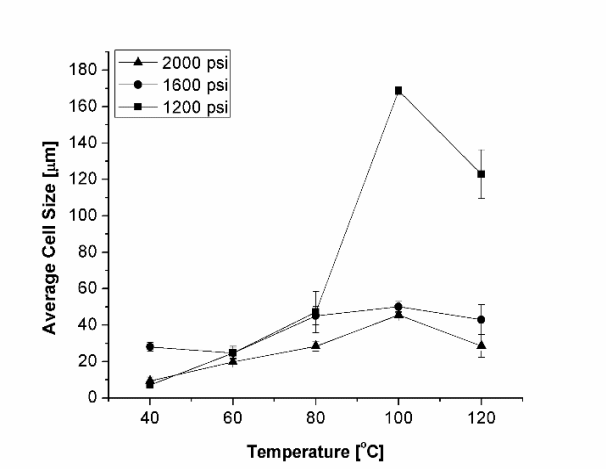

Figure 4.8. Effect of Foaming Temperature and Pressure on TPU Foam's Average Cell Size

In the TPU-CO_2 system, the mobility of HS chains within the crystalline domains was enhanced due to the plasticizing effect of CO_2 on the TPU matrix [11]. As the saturation pressure increased, the amount of HS crystalline domains would be promoted. This led to the release of CO_2 into the surrounding area and increased the degree of supersaturation within the proximity around the crystals for nucleation. Furthermore, the local stress fluctuation caused by the restricted molecular chain mobility in the soft segments of TPU would also contribute to the surge in

nucleating power of the polymer-gas system [11]. During the CO_2 foaming process, there are two competing phenomenon that would influence the crystal structure. On the one hand, the plasticizing effect of dissolved CO_2 would enhance the HS chain mobility, leading to a suppression of melting temperature that spanned a broad range as indicated in Figure 4.1. Therefore, the elevated temperature would melt the crystalline domains with lower degrees of perfection (i.e. with lower melting points). This would lead to a decrease in the number density of heterogeneous nucleating sites in the matrix. On the other hand, as shown in Figure 4.1, the presence of CO_2 also increased the amount of crystal with a higher degree of perfection (i.e. with a higher melting point), and that would in turn increase the number density of heterogeneous nucleating sites in the matrix. At higher saturation pressures (i.e. 1600 psi and 2000 psi), the latter phenomena occurred at a high level that was sufficient to compensate the melting of low perfection crystals. Therefore, increasing the foaming temperature did not suppress the nucleating power of the TPU-CO_2 system. However, when the saturation pressure was 1200 psi, the relatively lower level of plasticizing effect caused by smaller amount of dissolved CO_2 was insufficient to compensate melting the HS crystalline domains. This led to a decrease in the number density of heterogeneous nucleating sites in the matrix, and thereby resulted in a dramatic decrease in TPU foam's cell population density as the foaming temperature increased beyond 80°C.

Overall, this work demonstrated that higher saturation pressures would yield a wide processing window to fabricate TPU foams with uniformly distributed fine cells. This is desirable for a wide range of applications such as lightweight structural applications. At the other end of the spectrum, if the goal is to expand the functions of TPU foams by embedding functional fillers (e.g. nanotubes or hexagonal boron nitride) in the TPU matrix, bubble expansion during foaming can assist both the alignment and alter the networking of these functional fillers along the cell wall. In this context,

a uniform distribution of fine cells structure may not be the ideal morphology. In contrast, foaming TPU at a lower saturation pressure (e.g. 1200 psi) and fine tuning the foaming temperature to achieve an appropriate level of bubble expansion would be beneficial to filler alignment and thereby enhance TPU's multifunctional properties (e.g. mechanical, thermal, and electrical).

4.3 Conclusions

This phase reports the fabrication of TPU foams by batch foaming using supercritical carbon dioxide (CO_2). The effects of foaming temperature and saturation pressure on TPU's crystallization and foaming behaviors were studied. It was found that the enhanced crystallization during the CO_2 saturation stage of the batch foaming process could significantly influence TPU's foaming behavior. Morphologies of TPU foams prepared at lower saturation pressures (i.e. 1200 psi) and those at higher saturation pressures (i.e. 1600 psi and 2000 psi) were very different due to the variation in TPU's crystallization behaviors under different processing conditions. It is important to note that the HS crystals in TPU served as heterogeneous nucleating sites to promote its cell nucleating power. As the melting of TPU crystals spanned a wide range of temperatures, varying the foaming temperature would allow the tuning of the number of these heterogeneous nucleating sites. In other words, the elucidation of this mechanism would provide insights to developing new processing strategies to fabricated TPU foams with desired morphologies. On the one hand, a high supersaturation pressure will be used to fabricate TPU foams with uniformly distributed fine cells, while on the other hand, a lower saturation pressure would yield a strong dependence of bubble expansion to varying foaming temperatures. Such a processing window provides more flexibility for researchers or manufacturers to identify the optimal cell size, through foaming-assisted filler alignment, to promote specific multifunctional properties of TPU composite or nanocomposite foams.

Chapter 5
Parametric Study of Foam Morphology on Polymer Composite Foam's k_{eff}

5.1 Introduction

The effects of foaming temperature and pressure on TPU foam's morphology were studied in Chapter 4. It was found that the foaming behaviours at a lower saturation pressure (i.e. 1200 psi) and those at higher saturation pressures (i.e. 1600 psi and 2000 psi) were different due to the variation in crystallization behaviors of TPU under different processing conditions. In particular, a lower saturation pressure yields higher sensitivity of cell expansion to varying foaming temperatures. This suggests that foaming-assisted filler alignment in TPU composite foams would benefit from being conducted in such processing windows as it would provide researchers more flexibility to identify the optimal cell size to promote specific multifunctional properties of TPU composite or nanocomposite foams. However, in some cases, specific alignment has not been observed, but foaming would help to create a better thermal conductivity network. In this context, an experimental study was conducted using TPU-hexagonal boron nitride (hBN) composite foams by batch foaming as a case example.

5.2 Results and Discussion

5.2.1 hBN dispersion in TPU matrix

Figure 5.1 shows the SEM micrographs of TPU-hBN composites with different hBN contents. The uniform dispersion of hBN platelets can be clearly seen in all the blends. According to the analyses conducted using the Image J software, the lateral sizes of hBN platelets were

approximately 5-6 microns. Moreover, hBN platelets started network formation with hBN content increasing in the TPU matrix.

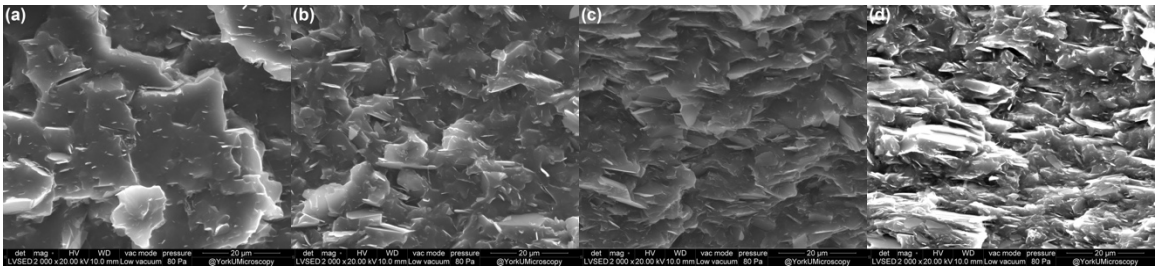

Figure 5.1. SEM Micrographs of TPU/hBN Composite with Different hBN Loadings: (a) 5 vol. %; (b) 10 vol. %; (c) 15 vol. %; and (d) 20 vol. %

5.2.2 Effect of Processing Conditions on Foaming Behaviors of TPU-hBN Composite

Figures 5.2(a) - (c) show the changes in the volume expansion ratios of TPU-hBN foams over time after the batch foaming process. Regardless of the saturation pressure, TPU-hBN foams prepared at lower temperatures (i.e. 20 and 40°C) shrank dramatically over the first hour but changed negligibly afterward, following the physical foaming process. In contrast, the volume expansion ratios of TPU foams prepared at 60°C or higher were virtually unchanged over time. This phenomenon was similar to changes in the volume expansion ratio of neat TPU foams. As discussed in the previous chapter, this diametrical reduction in TPU foam's volume expansion ratio over time could be attributed to the elastic recovery, which was due to the physical cross-links among the rigid segments and presence of the flexible segments in the thermoplastic elastomer. At lower foaming temperatures (i.e. 20 and 40°C), the TPU molecular chains had limited mobility, leading to a higher degree of volume recovery after foam expansion. At higher foaming temperatures (i.e. 60°C or higher) together with the plasticizing effect of CO_2, there was improved mobility of molecular chains around expanding cells. This, in turn, resulted in a more dimensionally stable foam structure.

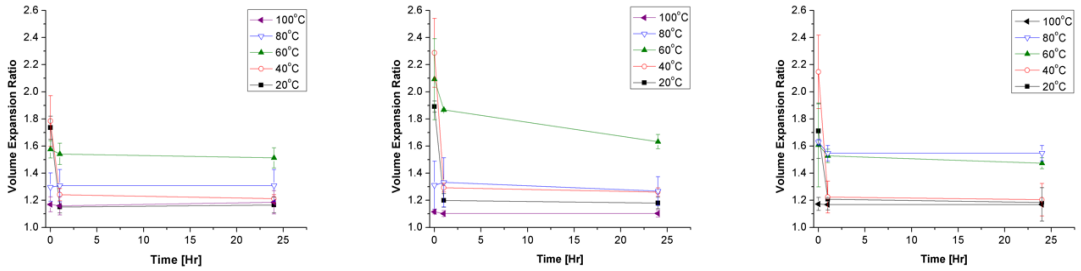

Figure 5.2. Effect of Foaming Temperature on the Change in TPU-hBN Composite Foam's Volume Expansion Ratio Under Ambient Conditions (Saturation Pressure:

(a) 1200 psi; (b) 1600 psi; and (c) 2000 psi)

Figure 5.3 shows the volume expansion ratio of TPU-hBN composites fabricated at different pressures and different temperatures measured after leaving them under ambient conditions for 24 hours. Regardless of the saturation pressure, it can be observed that there is an optimal temperature to get the highest volume expansion ratio of TPU-hBN composite foams (i.e. 60°C). However, the optimal temperature of TPU foams' morphology prepared at a saturation pressure of 2000 psi shifted to a higher temperature (i.e. 80°C). This is due to higher nucleation power and lower gas loss at higher saturation pressures compared to lower saturation pressures.

As the temperature increased from 20°C to 60°C, the elevated temperature caused greater flexibility of polymer matrix, which resulted in the expansion of TPU. However, when the foaming temperature further increased to 80°C, the excessive loss of a blowing agent at an elevated temperature contributed to the decrease in TPU-hBN foam's volume expansion ratio. Such observation was similar to the typical observation in neat TPU foams.

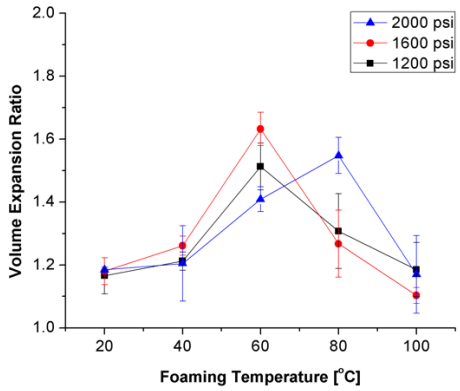

Figure 5.3. Effect of Foaming Temperature and Saturation Pressure on TPU-hBN Composite Foam's Volume Expansion

Parametric studies were conducted on various key processing parameters that govern the foaming process, including the saturation pressure (i.e. 1200, 1600, and 2000 psi) and foaming temperatures (i.e. 20, 40, 60, 80, 100, and 120°C). Figures 5.4 - 5.6 show the SEM micrographs of the foam morphology of TPU-hBN composite foams fabricated at different combinations of saturation pressure and temperature. Regardless of the saturation pressure, it can be observed that there was an optimal temperature at which to promote the cell size of the TPU-hBN composite foams. Furthermore, it is also apparent that the optimal temperature of TPU foams' morphology prepared at a saturation pressure of 2000 psi was different from those fabricated at lower saturation pressures. As expected, at a higher saturation pressure, the higher solubility of CO_2 would result in smaller cell size and higher cell density, as shown in Figures 5.7 and 5.8.

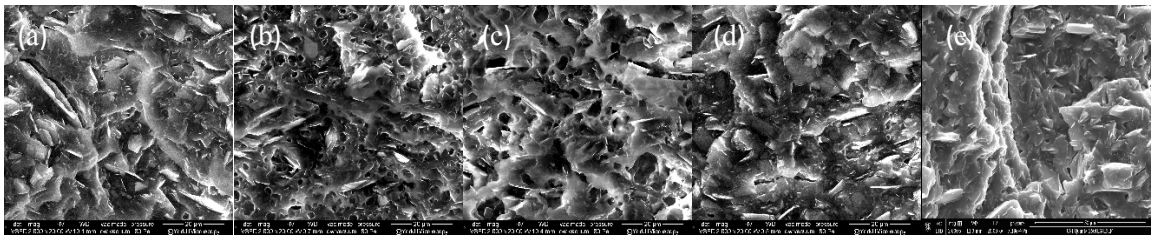

Figure 5.4. SEM Micrographs of TPU-hBN Foams Prepared at 1200 psi and Different Foaming Temperatures: (a) 20°C (b) 40°C; (c) 60°C; (d) 80°C; and (e) 100°C

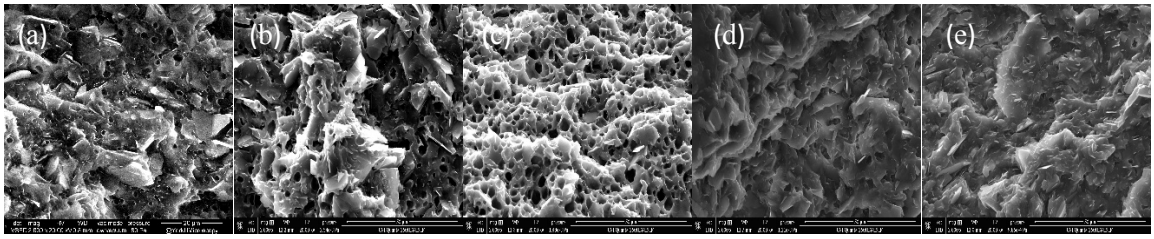

Figure 5.5. SEM Micrographs of TPU-hBN Foams Prepared at 1600 psi and Different Foaming Temperatures: (a) 20°C (b) 40°C; (c) 60°C; (d) 80°C; and (e) 100°C

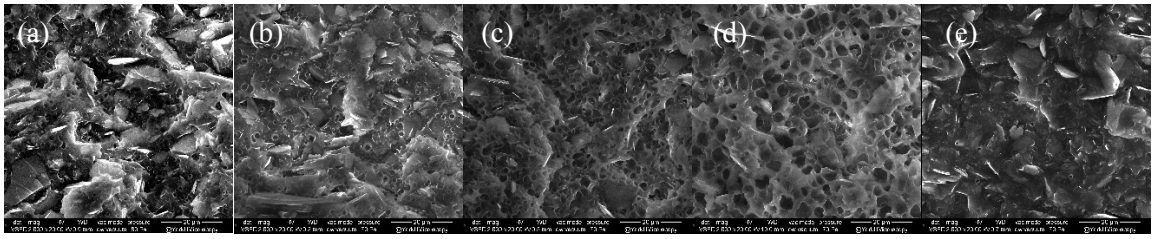

Figure 5.6. SEM Micrographs of TPU-hBN Foams Prepared at 2000 psi and Different Foaming Temperatures: (a) 20°C (b) 40°C; (c) 60°C; (d) 80°C; and (e) 100°C

By increasing the foaming temperature, molecular chain mobility increased. This resulted in a higher cell population density as shown in Figure 5.7. However, when the foaming temperature was higher than an optimal level, cell density decreased due to excessive gas loss. The aforementioned gradual temperature dependence of TPU's foam morphology was evidenced in the SEM micrographs of all TPU-hBN foams, except that the optimal temperature to get the highest cell population density was different for foams fabricated at a saturation pressure of 2000 psi (i.e. 80°C).

The average cell sizes of TPU-hBN composite foamed at various temperatures and pressures are shown in Figure 5.8. As can be observed, the cell sizes of TPU-hBN composite foams fabricated at 1200 psi and 1600 psi increased by increasing the temperature from 20°C to 60°C. When the foaming temperature further increased to 100°C, the average cell size decreased. As the foaming temperature increased, the increase in CO_2 diffusivity would promote cell expansion.

However, as the temperature continued to increase, the excessive gas loss to the surrounding environment would eventually lead to smaller cell sizes. However, the optimal temperature to promote the cell size for foams fabricated at 2000 psi was different from the others at lower saturation pressures (i.e. 80°C). In general, the cell size was considerably suppressed by adding hBN to TPU. It could be attributed to the rigidity of hBN which resulted in decreasing TPU flexibility.

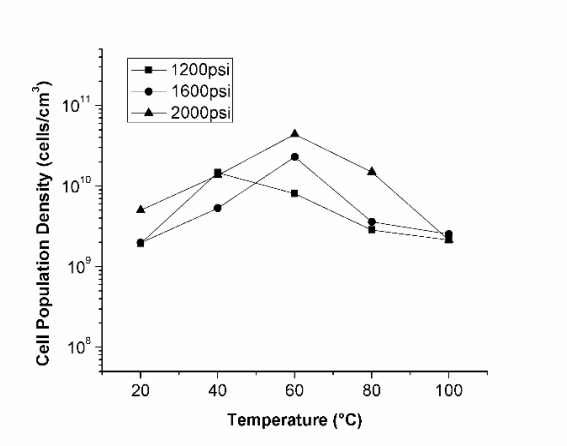

Figure 5.7. Effect of Foaming Temperature and Pressure on TPU-hBN Foam's Cell Population Density

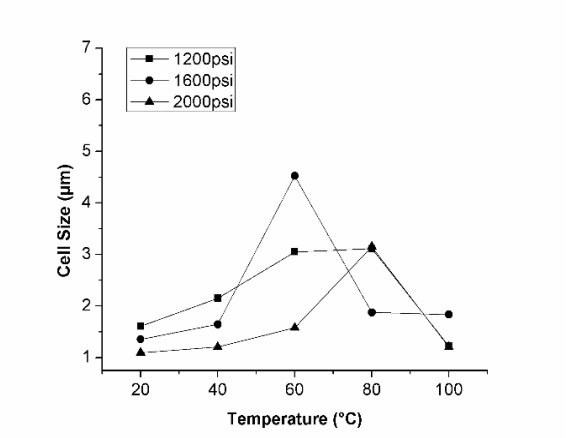

Figure 5.8. Effect of Foaming Temperature and Pressure on TPU-hBN Foam's Cell Population Density

5.2.3 Effect of Foaming Process on TPU-hBN Composite's k_{eff}

Figure 5.9 plots thermal conductivities as a function of filler loading. As hBN loading gradually increase, hBN platelets are able to interconnect and form a conductive network in the TPU matrix. This is more pronounced when the hBN loading increases to 15 vol.% or above. As can be seen in Figure 5.9, at very low filler loading (5-10 vol.%), there is low enhancement in composite's k_{eff}. At low hBN loading, the population density of hBN platelets is insufficient to establish a thermally conductive network in the TPU matrix. However, hBN platelets are able to form an interconnected network in the TPU matrix at a high hBN loading. A higher filler loading compromises low density, good processing ability, low cost, and flexibility. Since 15 vol.% hBN was the lowest loading that demonstrate obvious filler-to-filler interaction in SEM micrographs, this is used as the base case to evaluate the feasibility and effectiveness of foaming-assisted filler alignment to promote composite's k, especially with low filler loadings.

As aforementioned, foaming has the potential to align the filler along the cell walls to achieve better thermal conductivity. To further investigate the effect of foam morphology on TPU-hBN foam's k_{eff}, various foaming conditions were applied. Figure 5.10 shows the plot of k_{eff} as a function of temperature at different saturation pressures. Regardless of saturation pressure, the highest effective thermal conductivity was achieved at 20°C and 40°C. As discussed earlier, at these lower foaming temperatures, there is a dramatic decrease in TPU-hBN foam's volume expansion ratio over the first hour and a negligible change thereafter. This suggests that initial expansion at those lower temperatures improve thermal conductivity of the composite by forming a more interconnected thermal conductivity network, as shown in Figure 5.11. The initial expansion helps to enhance thermal conductivity network. Furthermore, elastic recovery at a lower saturation temperature results in lower volume expansion ratio and smaller cell sizes which

minimizes the thermal insulating of cells as shown in Figure 5.12. Moreover, elastic recovery makes the filler more connected and creates a better interconnected network.

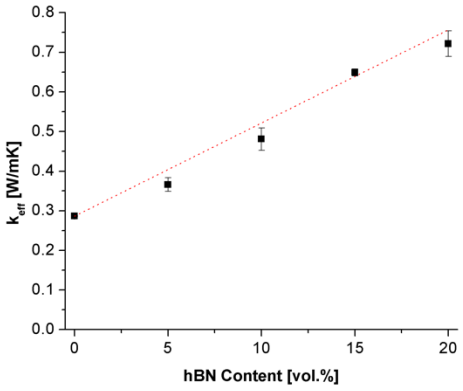

Figure 5.9. Effect of hBN Content on the k_{eff} of TPU-hBN composites

Figure 5.10 shows the foam structure of TPU-hBN composite fabricated at 1600psi and different saturation temperatures (i.e. 20, 60, and 80°C). TPU-hBN composite foam fabricated at lower saturation temperatures (i.e. 20 and 40°C) yielded better k_{eff} than those prepared at higher saturation temperatures due to initial expansion and elastic recovery. In contrast, samples showed a lowest k_{eff} at 60°C due to a high number of cells which act as insulators.

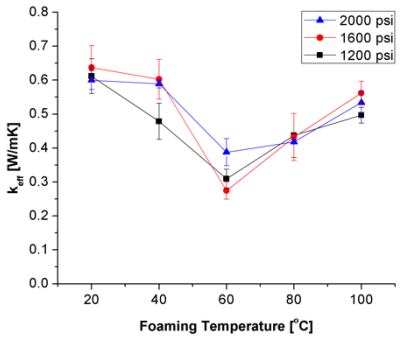

Figure 5.10. Effect of Foaming Temperature and Pressure on TPU-hBN Foam's k_{eff}

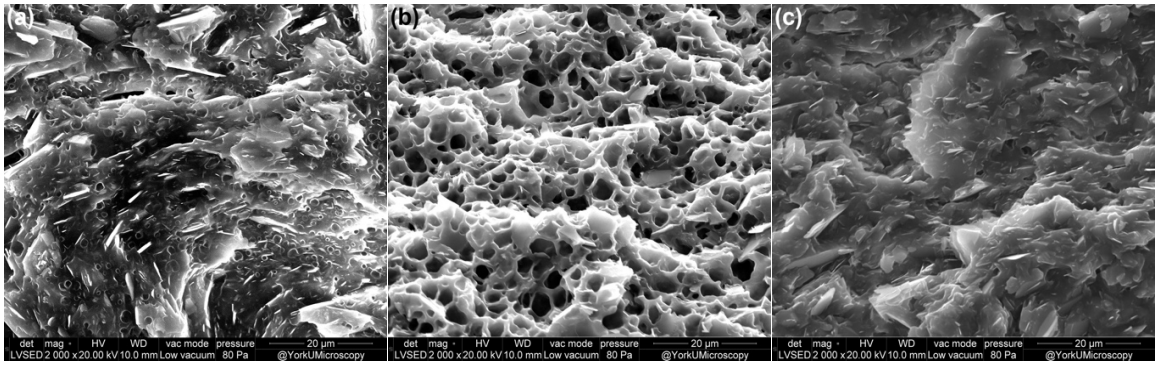

Figure 5.11. SEM Micrographs of Representative TPU-hBN Composite Foams Fabricated at Foaming Temperature and Pressure of (a) 20°C & 1600 psi; (b) 60°C & 1600 psi; and (c) 100°C & 1600 psi

Figure 5.13 shows the schematic of creating thermal conductivity paths by initial expansion of TPU-hBN composite foams. The initial expansion pushed the fillers in some way to create thermal conductivity paths. Then, TPU-hBN foam shrank dramatically over the first hour which led to smaller cells and diminished the insulating effect of cells. Moreover, it helped fillers to get closer and interconnected. Therefore, thermal conductivity of TPU-hBN foams prepared at the lower saturation temperatures was greater.

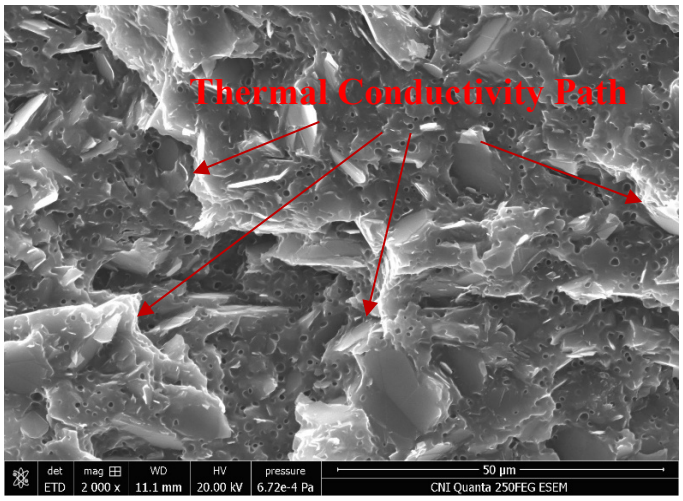

Figure 5.12. SEM Micrographs of TPU-hBN Foam Prepared at 1600 psi and 40°C

Figure 5.14 shows SEM micrographs of composite solid sample and foam sample fabricated at 100°C. In the solid sample, hBN platelets are more horizontal. At a higher saturation temperature (i.e. 100°C) mobility of molecular chains is enhanced due to the higher plasticizing effect of CO_2. As a result, foaming induced hBN platelets in different arrangements which resulted in better thermal conductivity, due to the high in-plane thermal conductivity of hBN platelets.

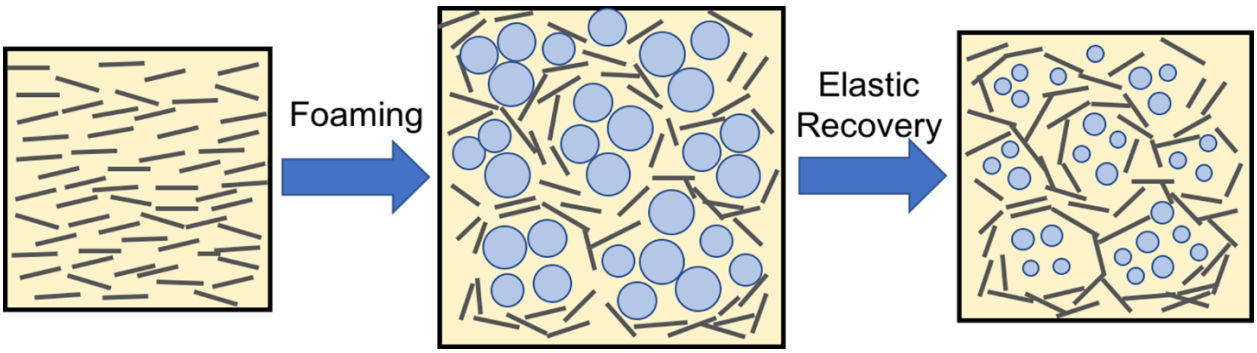

Figure 5.13. A Schematic Illustration of Microstructuring TPU-hBN Composites Through Low Temperature CO_2 Foaming

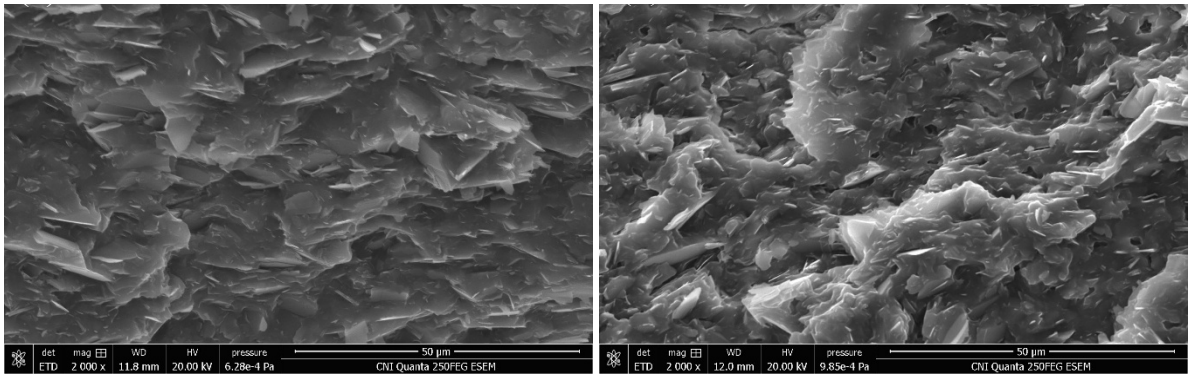

Figure 5.12. SEM Micrographs of (a) TPU-hBN Solid Sample and (b) TPU-hBN Foam Prepared at 1600 psi and 100°C

The effect of volume expansion ratio on TPU-hBN foam's k_{eff} is plotted in Figure 5.14. This shows that the best thermal conductivities were achieved between 10% and 20% foam expansion which is comparable with the solid counterparts. In contrast, expanding more than 20% is detrimental for TPU-hBN foam's k_{eff}. It can be observed, the best thermal conductivity is achieved

at lower temperatures which have high initial expansion and lower latter expansion. As a result, the initial expansion helps to establish a better interconnectivity filler network which results in higher thermal conductivity.

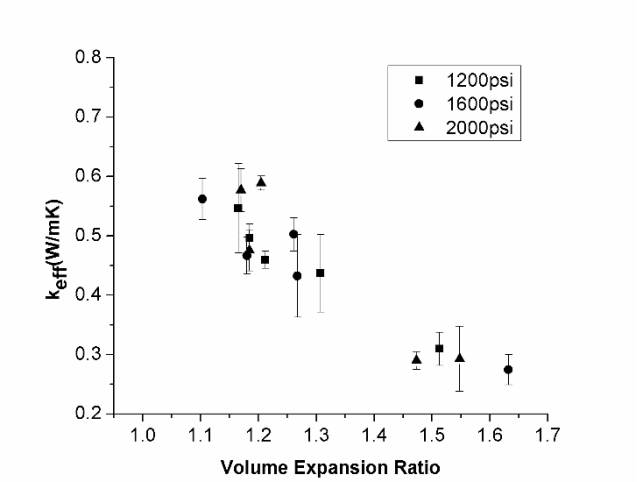

Figure 5.13. Effect of volume expansion ratio on TPU-hBN foam's k_{eff}

5.2.4 Effect of Cooling Time on TPU-hBN Composite's k_{eff}

The foaming structure was stabilized by immersing the samples in the ice bath for 30 seconds. However, at the lower temperatures, specimens started to expand more after taking them out of the ice bath and many big gas pockets appeared on the surface of the samples, as shown in Figures 5.16 and 5.17. This can be attributed to the high flexibility of the TPU matrix at this temperature which led to cell rupture. Therefore, by increasing the cooling time to five minutes, a better foam structure without any gas pockets was formed.

Figure 5.14. TPU-hBN Foamed at 1600 psi, 20°C and Shorter Cooling Time

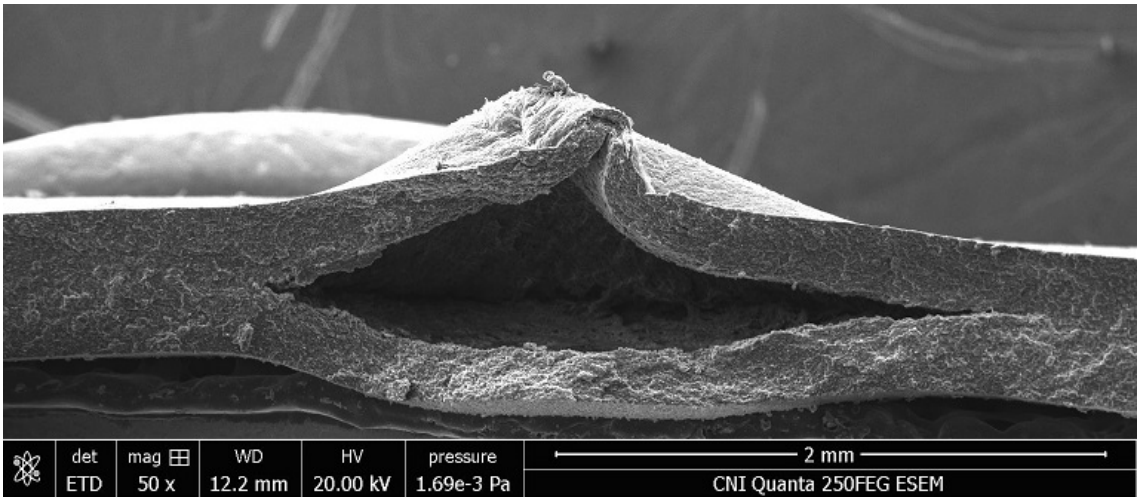

Figure 5.15. SEM Micrographs of TPU-hBN Foams Prepared at 1600 psi, 40°C and Shorter Cooling Time

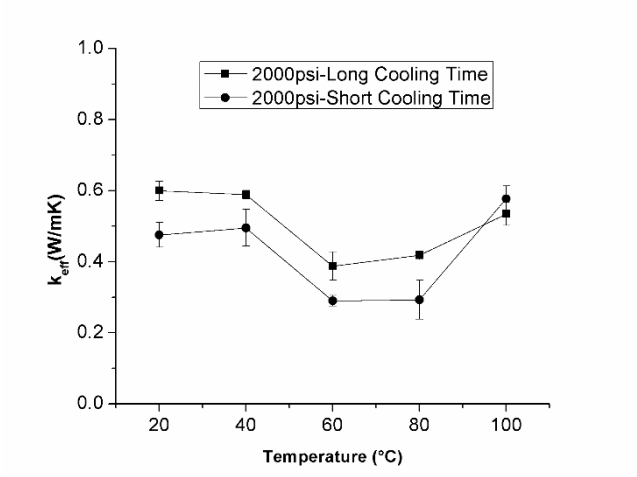

Figure 5.16. Effect of Cooling Time on TPU-hBN Composite's k_{eff}

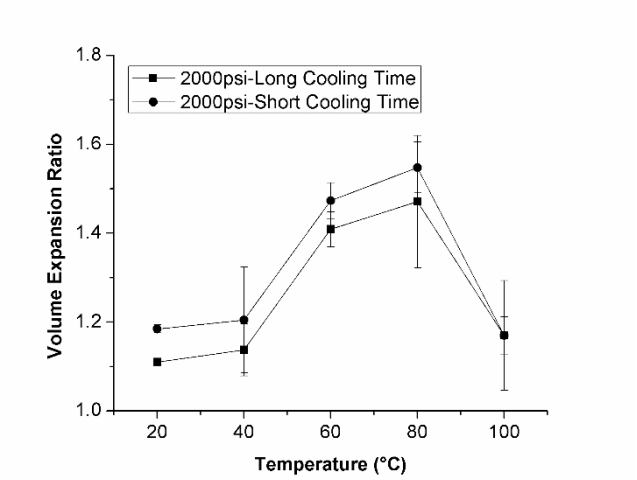

Figure 5.17. Effect of Cooling Time on TPU-hBN Composite's Volume Expansion Ratio

The effects of cooling time on TPU-hBN foam's k_{eff} and volume expansion ratio foamed at 2000 psi are shown in Figures 5.18 and 5.19 respectively. It is evident that samples fabricated at the shorter cooling time had lower thermal conductivity due to the presence of voids which act as thermal insulators in the polymer matrix. Therefore, by increasing the cooling time, arbitrary expansion and foam structure were achieved. To further investigate the effect of cooling times on TPU-hBN foam's k_{eff}, samples were fabricated at other pressures.

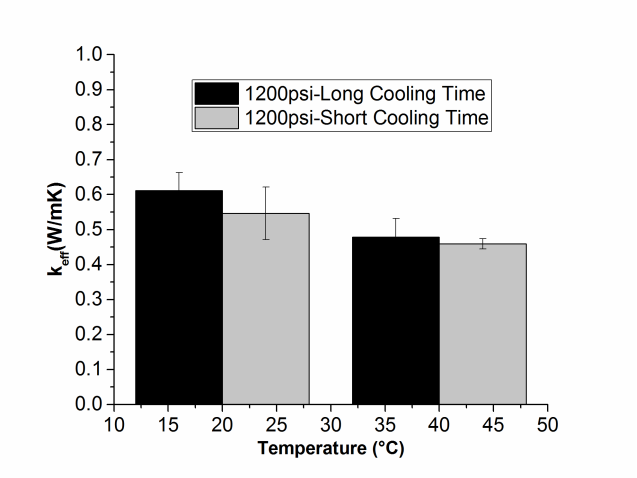

Figure 5.18. Effect of Cooling Time on TPU-hBN Composite's k_{eff} Fabricated at 1200 psi

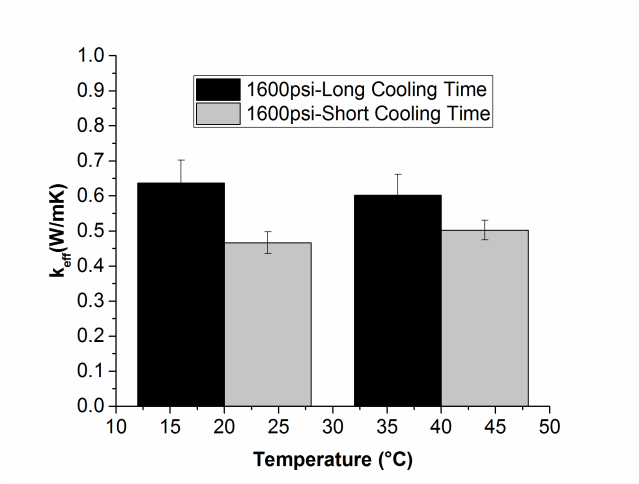

Figure 5.19. Effect of Cooling Time on TPU-hBN Composite's k_{eff} Fabricated at 2000 psi

Figures 5.19 and 5.20 illustrate the effect of cooling times on TPU-hBN foam's k_{eff} fabricated at 1200 psi and 1600 psi respectively. Regardless of the saturation pressure, samples fabricated with a longer cooling time had higher thermal conductivity due to the absence of gas pockets.

5.3 Conclusions

This study has successfully fabricated thermally conductive TPU-hBN composite foams with their effective thermal conductivity (k_{eff}) comparable to their solid counterparts. TPU foams with 15 vol. % filler loading were investigated. The thermal conductivity of TPU foams reached as high as 0.63 $W \cdot m^{-1} \cdot K^{-1}$ which is comparable to neat TPU (i.e. 0.64 $W \cdot m^{-1} \cdot K^{-1}$). The effects of foam morphologies on the TPU foam's k_{eff} were also investigated. It was shown that initial expansion at the lower temperatures led to improved thermal conductivity of the composite by forming a more interconnected thermal conductivity network. It also found that foaming induced fillers more vertically in polymer matrix at a higher temperature (i.e. 100°C) which resulted in high thermal conductivity. Moreover, the best thermal conductivities were achieved between 10% and 20% foam expansion which is comparable with their solid counterparts. In contrast, expanding more than 20%, which resulted in high volume fraction of thermally insulating air voids, is detrimental

for TPU-hBN foam's $k_{eff.}$ It was found that cooling time affects TPU-hBN foam's $k_{eff.}$ TPU-hBN foams fabricated at a shorter cooling time had lower k_{eff} due to the presence of big voids. This is attributed to the high flexibility of the TPU matrix at this temperature, which led to cell rupture.

In short, the findings of this research provide guidelines for researchers or manufacturers to design and fabricate lightweight, thermally conductive, TPU foams. Such new materials provide a potential way to deal with the challenges in heat management.

Chapter 6
Conclusion and Recommendations

6.1 Contribution

With the continuous technological advancement in the electronic industries, the power density, and thereby the amount of heat generation, of components have surged dramatically in the past decades. In this context, new materials that can contribute to thermal management of these components are of interests by the industry. While heat sinks have been used traditionally to promote the heat dissipation, the industry is urging for new thermally conductive materials that can be integrated in the electronic packaging in order to streamline the production process as well as to reduce the manufacturing cost and the components' sizes. In this context, polymeric material systems represent an important material family because of their existing uses in electronic packaging as well as the good processability.

Thermally conductive polymer material systems have been researched and developed extensively by researchers and the industry. Theoretically, thermally conductive composites are often fabricated by adding fillers with high thermal conductivity to polymer matrices such as metal, ceramic, and carbon-based fillers. Recent investigations on conducting polymer composites have led to some important disclosures regarding accessible thermal conductivity range and trends of changes in the conductivity parameter with variation in the loading level [144], structure of polymer matrix [145], and level of filler dispersion [146]. Recently, the concept of thermally conductive polymer composite foams has also been investigated and they [145] represent an interesting family of materials for thermal management applications.

The main goal of my thesis is to develop a conformable thermally conductive polymer composite. Thermoplastic polyurethane (TPU)- hexagonal boron nitride (hBN) composites foamed by batch foaming were studied as a case example. Physical foaming is proposed in this thesis as a potential route to induce filler alignment along the cell wall, and thereby to establish a thermally conductive network in the material system. However, there is a critical level of cell expansion to perfectly align the fillers around the expanded cells and further expansion would break the thermally conductive network and decrease TPU foam's k_{eff}. Therefore, an understanding of foam morphology is critical to the rational design of improved thermally conductive TPU foams.

First, a comprehensive experimental study was conducted to identify the foaming behaviors of TPU foams in order to identify appropriate processing windows that would offer flexibility to develop multifunctional TPU composite and nanocomposite foams. TPU foams were fabricated by batch foaming and subsequently be characterized. It was shown that by CO_2 foaming it was possible to produce TPU foams at relatively low temperatures (60°C). it also found that the cell size and cell density range is significantly wider at lower saturation pressures to varying foaming temperatures. This is due to the fact that there is a difference in crystallization behaviors of TPU at different saturation pressures. At lower saturation pressure, specifically, there are fewer crystals which can act as heterogeneous nucleating sites. While TPU foams usually yield extremely high cell population density and small cell size, by applying the appropriate foaming conditions, we prepared foams with a wide range cell size from 21 to 170 μm and cell population density from 105 to 108 pore/cm^3.

Second, these conditions have been used to investigate the foaming-assisted filler alignment in TPU composite and nanocomposite foams for tailoring the thermal conductivity. Thermally conductive thermoplastic polyurethane (TPU)-hexagonal boron nitride (hBN) composite foams

have been achieved with their k_{eff} comparable to their solid counterparts. The thermal conductivity of TPU foams reached as high as 0.63 $W \cdot m^{-1} \cdot K^{-1}$ which can be comparable to neat TPU (i.e. 0.64 $W \cdot m^{-1} \cdot K^{-1}$). The results of this research demonstrated that initial expansion at lower temperatures (i.e., 20 and 40°C) lead to improve thermal conductivity of composite by forming a more interconnected thermal conductivity networks. The results also indicated that foaming induced fillers more vertically in polymer matrix at higher temperature (i.e., 100°C) which resulted in high thermal conductivity. Moreover, the best thermal conductivities were achieved between 10% and 20% foam expansion which could be comparable with the solid counterparts. It was also found that cooling time is an effective parameter on TPU-hBN foam's k_{eff}. TPU-hBN foams fabricated in a shorter cooling time had lower k_{eff} due to presence of big voids. This can be attributed to the high flexibility of the TPU matrix at this temperature which leads to cell rupture.

6.2 Recommendations for Future Work

This thesis has investigated the effect of foaming on filler alignment to enhance the thermal conductivity of the polymer composites. However, nanofillers tend to aggregate which results in failing the filler to meet its purpose. Therefore, well dispersion of the filler in polymer matrix enhances the formation of conductive paths, resulting in better thermal conductivity. Hence for future work, it would be very interesting to systematically investigate using the surface treatment which can improve the dispersion of the filler in the polymer matrix by enhancing the compatibility between the filler and the matrix.

Another possible area of exploration, based on TPU-hBN foams generated from this research, is to evaluate the foam's heat dissipating performance which is really important in heat management applications. This study has focused on thermal conductivity and flexibility of the polymer composites. However, in order to reduce any thermal stresses, packaging material should

have a tailorable coefficient of thermal expansion (CTE) which could be matched to substrate materials. Moreover, in electronic packaging applications, packaging materials should have high electrical resistivity. Therefore, it will be interesting to evaluate other properties such as thermal expansion and dielectric properties in further studies.

Bibliography

[1] M. G. Pecht, L. T. Nguyen, E. B. Hakim, "'Plastic encapsulated microcircuits,'" *Eng. Mag.,* pp. 22-23, 1996.

[2] D. Bloor, A. Graham, E. J. Williams, P. J. Laughlin, and D. Lussey, "Metal-polymer composite with nanostructured filler particles and amplified physical properties," *Appl. Phys. Lett.*, vol. 88, no. 10, pp. 102-103, 2006.

[3] G. W. Lee, M. Park, J. Kim, J. I. Lee, and H. G. Yoon, "Enhanced thermal conductivity of polymer composites filled with hybrid filler," *Compos. Part A Appl. Sci. Manuf.*, vol. 37, no. 5, pp. 727–734, 2006.

[4] Z. Han and A. Fina, "Thermal conductivity of carbon nanotubes and their polymer nanocomposites: A review," *Prog. Polym. Sci.*, vol. 36, no. 7, pp. 914–944, 2011.

[5] H. Ishida and S. Rimdusit, "Very high thermal conductivity obtained by boron nitride-filled polybenzoxazine," *Thermochim. Acta*, vol. 320, no. 1–2, pp. 177–186, Nov. 1998.

[6] C. A. Martin, J. K. W. Sanler, m. S. P. Shaffer, M. K. Schwarz, W. bauhofer, K. Schulte, and A.H. Windle, "Formation of percolating networks in multi-wall carbon-nanotube-epoxy composites," *Compos. Sci. Technol.*, vol. 64, no. 15, pp. 2309–2316, 2004.

[7] D. Klempener; V. Sendijarevic, "Polymeric foams and foam technology," *Polymer (Guildf).*, vol. 2, no. 4, pp. 584, 2004.

[8] J. Vega-Baudrit, V. Navarro-Banon, P. Vázquez, and J. M. Martín-Martínez, "Addition of nanosilicas with different silanol content to thermoplastic polyurethane adhesives," *Int. J. Adhes. Adhes.*, vol. 26, no. 5, pp. 378–387, 2006.

[9] A. K. Mishra, P. R. Rajamohanan, G. B. Nando, and S. Chattopadhyay, "Structure-property of thermoplastic polyurethane-clay nanocomposite based on covalent and dual-modified laponite," *Adv. Sci. Lett.*, vol. 4, no. 1, pp. 65–73, 2011.

[10] S. Roy, S. K. Srivastava, J. Pionteck, and V. Mittal, "Mechanically and thermally enhanced multiwalled carbon nanotube-graphene hybrid filled thermoplastic polyurethane nanocomposites," *Macromol. Mater. Eng.*, vol. 300, no. 3, pp. 346–357, 2015.

[11] N. J. Hossieny, M. R. Barzegari, M. Nofar, S. H. Mahmood, and C. B. Park, "Crystallization of hard segment domains with the presence of butane for microcellular thermoplastic polyurethane foams," *Polym. (United Kingdom)*, vol. 55, no. 2, pp. 651–662, 2014.

[12] W. Michaeli and R. Heinz, "Foam extrusion of thermoplastic polyurethanes (TPU) using CO_2 as a blowing agent," *Macromol. Mater. Eng.*, vol. 284, no. 1, pp. 35–39, 2000.

[13] X. Tao, "Wearable electronics and photonics," *woodhead publishing,* 2005.

[14] S. Lam Po Tang, "Recent developments in flexible wearable electronics for monitoring applications," *Trans. Inst. Meas. Control*, vol. 29, no. 3–4, pp. 283–300, 2007.

[15] W. Zeng, L. Shu, Q. Li, S. Chen, F. Wang, and X. M. Tao, "Fiber-based wearable electronics: A review of materials, fabrication, devices, and applications," *Advanced Materials*, vol. 26, no. 31. pp. 5310–5336, 2014.

[16] M. Park, J. Im, M. Shin, Y. Min, J. Park, H. Cho, S. park, M.B. Shim, S. Jeon, D. Y. chung, J. bae, J. park, U. jeong, and K. Kim, "Highly stretchable electric circuits from a composite material of silver nanoparticles and elastomeric fibres," *Nat. Nanotechnol.*, vol. 7, no. 12, pp. 803–809, 2012.

[17] K. Cherenack, C. Zysset, T. Kinkeldei, N. Münzenrieder, and G. Tröster, "Woven electronic fibers with sensing and display functions for smart textiles," *Adv. Mater.*, vol. 22, no. 45, pp. 5178–5182, 2010.

[18] Z. Li and Z. L. Wang, "Air/liquid-pressure and heartbeat-driven flexible fiber nanogenerators as a micro/nano-power source or diagnostic sensor," *Adv. Mater.*, vol. 23, no. 1, pp. 84–89, 2011.

[19] K. Koski, A. Vena, L. Sydanheimo, L. Ukkonen, and Y. Rahmat-Samii, "Design and implementation of electro-textile ground planes for wearable UHF RFID patch tag antennas," *IEEE Antennas Wirel. Propag. Lett.*, vol. 12, no. N/A, pp. 964–967, 2013.

[20] J. Y. Wong, J. McDonald, M. Taylor-Pinney, D. I. Spivak, D. L. Kaplan, and M. J. Buehler, "Materials by design: Merging proteins and music," *Nano Today*, vol. 7, no. 6. pp. 488–495, 2012.

[21] R. Paradiso, G. Loriga, and N. Taccini, "Wealthy, a wearable healthcare system: new frontier on e-textile," *J. Telecomunications Inf. Technol.*, vol. 4, no. N/A, pp. 105–113, 2005.

[22] L. Gatzoulis and I. Iakovidis, "Wearable and portable ehealth systems," *IEEE Engineering in Medicine and Biology Magazine*, vol. 26, no. 5. pp. 51–56, 2007.

[23] D. L. Mann, M. A. Acker, M. Jessup, H. N. Sabbah, R. C. Starling, and S. H. Kubo, "Clinical evaluation of the corcap cardiac support device in patients with dilated cardiomyopathy," *Ann. Thorac. Surg.*, vol. 84, no. 4, pp. 1226–1235, 2007.

[24] C. Zweben, "Advances in composite materials for thermal management in electronic," *JOM J. Miner. Met. Mater. Soc.*, vol. 50, no. 6, pp. 47–51, 1998.

[25] X. C. Tong, "Advanced materials for thermal management of electronic packaging", *Springer*, 2011.

[26] X. C. Tong, "Advanced materials for thermal management of electronic packaging," *Adv. Mater.*, vol. 30, no. Chung 2003, pp. 201–232, 2011.

[27] C. Zweben, "Metal-matrix composites for electronic packaging," *JOM*, vol. 44, no. 7, pp. 15–23, 1992.

[28] C. Zweben, "Advanced electronic packaging materials," *Adv. Mater. Process.*, vol. 163, no. 10, pp. 33–37, 2005.

[29] B. S. William B. Johnson, "Diamond/Al metal matrix composites formed by the pressureless metal infiltration S," *J. J. Mater. Res.*, vol. 8, no. 5, pp. 1169-1173, 1993.

[30] C. P. Wong and R. S. Bollampally, "Thermal conductivity, elastic modulus, and coefficient of thermal expansion of polymer composites filled with ceramic particles for electronic packaging," *J. Appl. Polym. Sci.*, vol. 74, no. 14, pp. 3396–3403, 1999.

[31] E. Lee and S. Lee, "Enhanced thermal conductivity of polymer matrix composite via high

solids loading of aluminum nitride in epoxy resin," *J.Am.Ceram.Soc.*, vol. 91, no. 23504, pp. 1169–1174, 2008.

[32] W. Kim, J. W. Bae, I. D. Choi, and Y. S. Kim, "Thermally conductive EMC (epoxy molding compound) for microelectronic encapsulation," *Polym. Eng. Sci.*, vol. 39, no. 4, pp. 756–766, 1999.

[33] S. Rimdusit and H. Ishida, "Development of new class of electronic packaging materials based on ternary systems of benzoxazine, epoxy, and phenolic resins," *Polymer (Guildf).*, vol. 41, no. 22, pp. 7941–7949, 2000.

[34] C. L. Choy, "Thermal conductivity of polymers," *Polymer*, vol. 18, no. 10. pp. 984–1004, 1977.

[35] A. Henry, "Thermal trasport in polymers," *Annu. Rev. Heat Transf.*, vol. 17, no. N/A, pp. 485–520, 2014.

[36] S. Shen, A. Henry, J. Tong, R. Zheng, and G. Chen, "Polyethylene nanofibres with very high thermal conductivities," *Nat. Nanotechnol.*, vol. 5, no. 4, pp. 251–255, 2010.

[37] C. L. Choy, Y. W. Wong, G. W. Yang, and T. Kanamoto, "Elastic modulus and thermal conductivity of ultradrawn polyethylene," *J. Polym. Sci. Part B Polym. Phys.*, vol. 37, no. 23, pp. 3359–3367, 1999.

[38] C. L. Choy, W. H. Luk, and F. C. Chen, "Thermal conductivity of highly oriented polyethylene," *Polymer (Guildf).*, vol. 19, no. 2, pp. 155–162, 1978.

[39] C. L. Choy, "Thermal conductivity of polymers," *Polymer*, vol. 18, no. 10. pp. 984–1004, 1977.

[40] Y. P. Mamunya, H. Zois, L. Apekis, and E. V. Lebedev, "Influence of pressure on the electrical conductivity of metal powders used as fillers in polymer composites," *Powder Technol.*, vol. 140, no. 1–2, pp. 49–55, 2004.

[41] Y. P. Mamunya, V. V. Davydenko, P. Pissis, and E. V. Lebedev, "Electrical and thermal conductivity of polymers filled with metal powders," *Eur. Polym. J.*, vol. 38, no. 9, pp. 1887–1897, 2002.

[42] W. Y. Zhou, S. H. Qi, H. Z. Zhao, and N. L. Liu, "Thermally conductive silicone rubber reinforced with boron nitride particle," *Polym. Compos.*, vol. 28, no. 1, pp. 23–28, 2007.

[43] D. D. . Chung, "Materials for thermal conduction," *Appl. Therm. Eng.*, vol. 21, no. 16, pp. 1593–1605, 2001.

[44] J. Jordan, K. I. Jacob, R. Tannenbaum, M. A. Sharaf, and I. Jasiuk, "Experimental trends in polymer nanocomposites - A review," *Materials Science and Engineering A*, vol. 393, no. 1–2. pp. 1–11, 2005.

[45] X. Huang, P. Jiang, and T. Tanaka, "A review of dielectric polymer composites with high thermal conductivity," *IEEE Electr. Insul. Mag.*, vol. 27, no. 4, pp. 8–16, 2011.

[46] Y. P. Mamunya, H. Zois, L. Apekis, and E. V. Lebedev, "Influence of pressure on the electrical conductivity of metal powders used as fillers in polymer composites," *Powder Technol.*, vol. 140, no. 1–2, pp. 49–55, 2004.

[47] F. Danes, B. Garnier, and T. Dupuis, "Predicting, measuring, and tailoring the transverse thermal conductivity of composites from polymer matrix and metal filler," *Int. J.*

Thermophys., vol. 24, no. 3, pp. 771–784, 2003.

[48] D. M. Bigg, "Thermal conductivity of heterophase polymer compositions," *Adv. Polym. Sci.*, vol. 119, no. N/A, pp. 1–30, 1995.

[49] X. Xu, M. M. Thwe, C. Shearwood, and K. Liao, "Mechanical properties and interfacial characteristics of carbon-nanotube-reinforced epoxy thin films," *Appl. Phys. Lett.*, vol. 81, no. 15, pp. 2833–2835, 2002.

[50] E. Kymakis, I. Alexandou, and G. A. . Amaratunga, "Single-walled carbon nanotube–polymer composites: electrical, optical and structural investigation," *Synth. Met.*, vol. 127, no. 1–3, pp. 59–62, 2002.

[51] R. Haggenmueller, C. Guthy, J. R. Lukes, J. E. Fischer, and K. I. Winey, "Single wall carbon nanotube/polyethylene nanocomposites: Thermal and electrical conductivity," *Macromolecules*, vol. 40, no. 7, pp. 2417–2421, 2007.

[52] R. Kochetov, T. Andritsch, U. Lafont, P. H. F. Morshuis, S. J. Picken, and J. J. Smit, "Thermal behaviour of epoxy resin filled with high thermal conductivity nanopowders," in *IEEE Electrical Insulation Conference* , pp. 524–528, 2009.

[53] M. Okamoto, P. H. Nam, P. Maiti, T. Kotaka, T. Nakayama, M. Takada, M. Ohshima, A. Usuki, N. Hasegawa, and H. Okamoto, "Biaxial Flow-Induced Alignment of Silicate Layers in Polypropylene/Clay Nanocomposite Foam," *Nano Lett.*, vol. 1, no. 9, pp. 503–505, 2001.

[54] E. H. Weber, M. L. Clingerman, and J. A. King, "Thermally conductive nylon 6,6 and polycarbonate based resins. II. Modeling," *J. Appl. Polym. Sci.*, vol. 88, no. 1, pp. 123–130, 2003.

[55] M. Roy, J. K. Nelson, R. K. Maccrone, L. S. Schadler, C. W. Reed, and R. Keefe, "Polymer nanocomposite dielectrics-the role of the interface," *Dielectr. Electr. Insul. IEEE Trans.*, vol. 12, no. 4, pp. 629–643, 2005.

[56] E. H. Weber, M. L. Clingerman, and J. A. King, "Thermally conductive nylon 6,6 and polycarbonate based resins. I. Synergistic effects of carbon fillers," *J. Appl. Polym. Sci.*, vol. 88, no. 1, pp. 112–122, 2003.

[57] H. Chen, V. V. Ginzburg, J. Yang, Y. yang, W. Liu, Y. Huang, L. Du, and B. Chen, "Thermal conductivity of polymer-based composites: Fundamentals and applications," *Progress in Polymer Science*, vol. 59, no. N/A, pp. 41-85, 2015.

[58] Y. Xu and D. D. L. Chung, "Increasing the thermal conductivity of boron nitride and aluminum nitride particle epoxy-matrix composites by particle surface treatments," *Compos. Interfaces*, vol. 7, no. 4, pp. 243–256, 2000.

[59] S. N. Leung, M. O. Khan, H. Naguib, and F. Dawson, "Multifunctional polymer nanocomposites with uniaxially aligned liquid crystal polymer fibrils and graphene nanoplatelets," *Appl. Phys. Lett.*, vol. 104, no. 8, pp. 081904, 2014.

[60] K. Yang and M. Gu, "Enhanced thermal conductivity of epoxy nanocomposites filled with hybrid filler system of triethylenetetramine-functionalized multi-walled carbon nanotube/silane-modified nano-sized silicon carbide," *Compos. Part A Appl. Sci. Manuf.*, vol. 41, no. 2, pp. 215–221, 2010.

[61] M. A. Vadivelu, C. R. Kumar, and G. M. Joshi, "Polymer composites for thermal

management: a review," *Compos. Interfaces*, vol. 23, no.9, pp. 847-872, 2016.

[62] X. Lu, G. Xu, P. G. Hofstra, and R. C. Bajcar, "Moisture-absorption, dielectric relaxation, and thermal conductivity studies of polymer composites," *J. Polym. Sci. Part B Polym. Phys.*, vol. 36, no. 13, pp. 2259–2265, 1998.

[63] E. K. Sichel, R. E. Miller, M. S. Abrahams, and C. J. Buiocchi, "Heat capacity and thermal conductivity of hexagonal pyrolytic boron nitride," *Phys. Rev. B*, vol. 13, no. 10, pp. 4607–4611, 1976.

[64] K. C. Yung and H. Liem, "Enhanced thermal conductivity of boron nitride epoxy-matrix composite through multi-modal particle size mixing," *J. Appl. Polym. Sci.*, vol. 106, no. 6, pp. 3587–3591, 2007.

[65] C. Raman and P. Meneghetti, "Boron nitride finds new applications in thermoplastic compounds," *Plast. Addit. Compd.*, vol. 10, no. 3, pp. 26-31, 2008.

[66] W. Shockley and H. J. Queisser, "Detailed balance limit of efficiency of p-n junction solar cells," *J. Appl. Phys.*, vol. 32, no. 3, pp. 510–519, 1961.

[67] C. A. Martin, J. K. W. Sandler, M. S. P. Shaffer, M. k. Schawrz, W. Bauhofer, K. Schulte, A. H. Windle, "Formation of percolating networks in multi-wall carbon-nanotube-epoxy composites," *Compos. Sci. Technol.*, vol. 64, no. 15, pp. 2309–2316, 2004.

[68] N. Tsutsumi, S. Kizu, W. Sakai, and T. Kiyotsukuri, "Thermal diffusivity study of polystyrene/poly(vinyl methyl ether) blends by flash radiometry," *J. Polym. Sci. Part B Polym. Phys.*, vol. 35, no. 12, pp. 1869–1876, 1997.

[69] C. Park, J. Wilkinson, S. Banda, Z. Ounaies, K. E. Wise, G. Sauti, P. T. Lillehei, and J. S. Harrison,"Aligned single-wall carbon nanotube polymer composites using an electric field," *J. Polym. Sci. Part B Polym. Phys.*, vol. 44, no. 12, pp. 1751–1762, 2006.

[70] T. Kimura, H. Ago, M. Tobita, S. Ohshima, M. Kyotani, and M. Yumura, "Polymer composites of carbon nanotubes aligned by a magnetic field," *Adv. Mater.*, vol. 14, no. 19, pp. 1380–1383, 2002.

[71] A. Yu, P. Ramesh, X. Sun, E. Bekyarova, M. E. Itkis, and R. C. Haddon, "Enhanced thermal conductivity in a hybrid graphite nanoplatelet - carbon nanotube filler for epoxy composites," *Adv. Mater.*, vol. 20, no. 24, pp. 4740–4744, 2008.

[72] H. Ding, Y. Guo, and S. N. Leung, "Development of thermally conductive polymer matrix composites by foaming-assisted networking of micron- and submicron-scale hexagonal boron nitride," *J. Appl. Polym. Sci.*, vol. 133, no. 4, 2016.

[73] C. C. Teng, C. C. M. Ma, K. C. Chiou, and T. M. Lee, "Synergetic effect of thermal conductive properties of epoxy composites containing functionalized multi-walled carbon nanotubes and aluminum nitride," *Compos. Part B Eng.*, vol. 43, no. 2, pp. 265–271, 2012.

[74] K. C. Yung, J. Wang, and T. M. Yue, "Thermal management for boron nitride filled metal core printed circuit board," *J. Compos. Mater.*, vol. 42, no. 1, pp. 2615–2627, 2008.

[75] R. Kochetov, "Thermal and electrical properties of nanocomposites, including material processing,"*Doctoral thesis*, 2012.

[76] B. Lee and G. Dai, "Influence of interfacial modification on the thermal conductivity of polymer composites," *J. Mater. Sci.*, vol. 44, no. 18, pp. 4848–4855, 2009.

[77] C. P. Wong, "Effect of interface on thermal conductivity of polymer composite," *Proc. Electron. Components Technol.*, vol. 2, no. 55, pp. 1451–1454, 2005.

[78] C. Zeng, X. Han, L. J. Lee, K. W. Koelling, and D. L. Tomasko, "Polymer-clay nanocomposite foams prepared using carbon dioxide," *Adv. Mater.*, vol. 15, no. 20, pp. 1743–1747, 2003.

[79] R. Everett, P. Matic, D. Harveyii, and a Kee, "The microstructure and mechanical response of porous polymers," *Mater. Sci. Eng. A*, vol. 249, no. 1–2, pp. 7–13, 1998.

[80] C. B. Park and N. P. Suh, "Rapid polymer/gas solution formation for continuous production of microcellular plastics," *J. Manuf. Sci. Eng. Trans. ASME*, vol. 118, no. 4, pp. 639–645, 1996.

[81] C. B. Park, D. F. Baldwin, and N. P. Suh, "Effect of the pressure drop rate on cell nucleation in continuous processing of microcellular polymers," *Polym. Eng. Sci.*, vol. 35, no. 5, pp. 432–440, 1995.

[82] M. J. Molina and F. S. Rowland, "Stratospheric sink for chlorofluoromethanes: chlorine atomc-atalysed destruction of ozone," *Nature*, vol. 249, no. 5460, pp. 810–812, 1974.

[83] A. Sekiya and S. Misaki, "The potential of hydrofluoroethers to replace CFCs, HCFCs and PFCs," *J. Fluor. Chem.*, vol. 101, no. 2, pp. 215–221, 2000.

[84] D. Eaves, "Polyolefin foams," in *Handbook of polymer foams, rapra*, pp. 173–205, 2004.

[85] A. K. Nema, A. V. Deshmukh, K. Palanivelu, S. K. Sharma, and T. Malik, "Effect of exo- and endothermic blowing and wetting agents on morphology, density and hardness of thermoplastic polyurethanes foams," *J. Cell. Plast.*, vol. 44, no. 4, pp. 277–292, 2008.

[86] X. Qin, M. R. Thompson, and A. N. Hrymak, "Rheology studies of foam flow during injection mold filling," *Polym. Eng. Sci.*, vol. 47, no. 4, pp. 522–529, 2007.

[87] D. Eaves, "Handbook of polymer foams," *Rapra Technol.*, 2004.

[88] M. R. Barzegari, J. Yao, and D. Rodrigue, "Compression molding of polyethylene foams under a temperature gradient: Morphology and flexural modulus," *Cell. Polym.*, vol. 28, no. 4, pp. 237–248, 2009.

[89] J. Yao, M. Reza Barzegari, and D. Rodrigue, "Polyethylene foams produced under a temperature gradient with expancel and blends thereof," *Cell. Polym.*, vol. 29, no. 5, pp. 259–282, 2010.

[90] L. Whinnery, S. Goods, and B. Even, "Expancel foams: Fabrication and characterization of a new reduced density cellular material for structural applications," *Sandia National Labs,* no. SAND2000-8217, 2000.

[91] Y. W. Kim, S. H. Kim, H. D. Kim, and C. B. Park, "Processing of closed-cell silicon oxycarbide foams from a preceramic polymer," *J. Mater. Sci.*, vol. 39, no. 18, pp. 5647–5652, 2004.

[92] M. A. Vadivelu, C. R. Kumar, and G. M. Joshi, "Polymer composites for thermal management: a review," *Compos. Interfaces*, vol. 23, no. 9, pp. 847–872, 2016.

[93] H. D. Kim, J. H. Huh, E. Y. Kim, and C. C. Park, "Comparison of properties of thermoplastic polyurethane elastomers with two different soft segments," *J. Appl. Polym. Sci.*, vol. 69, no. 7, pp. 1349–1355, 1998.

[94] S. L. Cooper and A. V. Tobolsky, "Properties of linear elastomeric polyurethanes," *J. Appl. Sci.,* vol. 10, no. 12, pp. 1837-1844, 1966.

[95] F. Gao, "Advances in polymer nanocomposites: Types and applications," *Woodhead Publishing*, 2012.

[96] R. Bonart and E. H. Muller, "Phase separation in urethane elastomers as iudged by low-angle X-Ray scattering. I. Fundamentals," *J. Macromol. Sci. Part B*, vol. 10, no. 1, pp. 177–189, 1974.

[97] A. Eceiza *et al.*, "Structure-property relationships of thermoplastic polyurethane elastomers based on polycarbonate diols," *J. Appl. Polym. Sci.*, vol. 108, no. 5, pp. 3092–3103, 2008.

[98] B. K. Kim, Y. J. Shin, S. M. Cho, and H. M. Jeong, "Shape-memory behavior of segmented polyurethanes with an amorphous reversible phase: the effect of block length and content," *J. Polym. Sci. Part B Polym. Phys.*, vol. 38, no. 20, pp. 2652–2657, 2000.

[99] B. Finnigan, P. Halley, K. Jack, A. Mcdowell, R. Truss, P. casey, R. Knott, D. Martin, "Effect of the average soft-segment length on the morphology and properties of segmented polyurethane nanocomposites," *J. Appl. Polym. Sci.*, vol. 102, no. 1, pp. 128–139, 2006.

[100] P. R. Laity, J. E. taylor, S. S. Wong, P. Khunkamchoo, M. Cable, G. T. andrews, A. F. Johnson, R. E. cameron, "Morphological changes in thermoplastic polyurethanes during heating," *J. Appl. Polym. Sci.*, vol. 100, no. 1, pp. 779–790, 2006.

[101] J. Silva, D. Meltzer, J. Liu, M. Cox, and J. Maia, "The influence of thermo-mechanical history on structure development of elastomeric and amorphous glass thermoplastic polyurethanes," *Polym. Eng. Sci.*, vol. 54, no. 6, pp. 1383–1393, 2014.

[102] L. B. Liu, M. Sumita, and K. Miyasaka, "Characterization of fatigue of segmented polyurethane by using thermoluminescence and pulse NMR," *J. Macromol. Sci. Part B*, vol. 28, no. 3–4, pp. 309–327, 1989.

[103] R. W. Seymour and S. L. Cooper, "Thermal analysis of polyurethane block polymers," *Macromolecules*, vol. 6, no. 1, pp. 48–53, 1973.

[104] R. W. Seymour, G. M. Estes, and S. L. Cooper, "Infrared studies of segmented polyurethan elastomers. I. Hydrogen bonding," *Macromolecules*, vol. 3, no. 5, pp. 579–583, 1970.

[105] L. Ning, W. De-Ning, and Y. Sheng-Kang, "Crystallinity and hydrogen bonding of hard segments in segmented poly(urethane urea) copolymers," *Polymer (Guildf).*, vol. 37, no. 16, pp. 3577–3583, 1996.

[106] S. B. Clough and N. S. Schneider, "Structural studies on urethane elastomers," *J. Macromol. Sci. Part B*, vol. 2, no. 4, pp. 553–566, 1968.

[107] X. Lu, Y. Wang, and X. Wu, "Study of hydrogen bonds in polyester-polyurethanes by solution n.m.r.," *Polymer (Guildf).*, vol. 35, no. 11, pp. 2315–2320, 1994.

[108] A. Saiani, A. Novak, L. Rodier, G. Eeckhaut, J. W. Leenslag, and J. S. Higgins, "Origin of multiple melting endotherms in a high hard block content polyurethane: Effect of annealing temperature," *Macromolecules*, vol. 40, no. 20, pp. 7252–7262, 2007.

[109] A. Frick and A. Rochman, "Characterization of TPU-elastomers by thermal analysis (DSC)," *Polym. Test.*, vol. 23, no. 4, pp. 413–417, 2004.

[110] Y. Yanagihara, N. Osaka, S. Murayama, and H. Saito, "Thermal annealing behavior and

structure development of crystalline hard segment domain in a melt-quenched thermoplastic polyurethane," *Polym. (United Kingdom)*, vol. 54, no. 8, pp. 2183–2189, 2013.

[111] R. E. Camargo, C. W. Macosko, M. Tirrell, and S. T. Wellinghoff, "Phase separation studies in RIM polyurethanes catalyst and hard segment crystallinity effects," *Polymer (Guildf).*, vol. 26, no. 8, pp. 1145–1154, 1985.

[112] J. Vega-Baudrit, V. Navarro-Bañón, P. Vázquez, and J. M. Martín-Martínez, "Addition of nanosilicas with different silanol content to thermoplastic polyurethane adhesives," *Int. J. Adhes. Adhes.*, vol. 26, no. 5, pp. 378–387, 2006..

[113] P. Wagener, S. Faramarzi, A. Schwenke, R. Rosenfeld, and S. Barcikowski, "Photoluminescent zinc oxide polymer nanocomposites fabricated using picosecond laser ablation in an organic solvent," *Appl. Surf. Sci.*, vol. 257, no. 16, pp. 7231–7237, 2011.

[114] W. Chen and X. Tao, "Production and characterization of polymer nanocomposite with aligned single wall carbon nanotubes," *Appl. Surf. Sci.*, vol. 252, no. 10, pp. 3547–3552, 2006.

[115] R. Zhang, H. Deng, R. valenca, J. Jin, Q. Fu, E. Bilotti, and T. Peijs, "Strain sensing behaviour of elastomeric composite films containing carbon nanotubes under cyclic loading," *Compos. Sci. Technol.*, vol. 74, no. N/A, pp. 1–5, 2013.

[116] P. C. Ma, N. A. Siddiqui, G. Marom, and J. K. Kim, "Dispersion and functionalization of carbon nanotubes for polymer-based nanocomposites: A review," *Compos. Part A Appl. Sci. Manuf.*, vol. 41, no. 10, pp. 1345–1367, 2010.

[117] A. Hirsch, "Functionalization of single-walled carbon nanotubes," *Angewandte Chemie - International Edition*, vol. 41, no. 11. pp. 1853–1859, 2002.

[118] K. Balasubramanian and M. Burghard, "Chemically functionalized carbon nanotubes," *Small*, vol. 1, no. 2. pp. 180–192, 2005.

[119] D. Tasis, N. Tagmatarchis, A. Bianco, and M. Prato, "Chemistry of carbon nanotubes.," *Chem. Rev.*, vol. 106, no. 3, pp. 1105–36, 2006.

[120] H. Quan, B. qing Zhang, Q. Zhao, R. K. K. Yuen, and R. K. Y. Li, "Facile preparation and thermal degradation studies of graphite nanoplatelets (GNPs) filled thermoplastic polyurethane (TPU) nanocomposites," *Compos. Part A Appl. Sci. Manuf.*, vol. 40, no. 9, pp. 1506–1513, 2009.

[121] D. A. Nguyen, Y. R. Lee, A. V. Raghu, H. M. Jeong, C. M. Shin, and B. K. Kim, "Morphological and physical properties of a thermoplastic polyurethane reinforced with functionalized graphene sheet," *Polym. Int.*, vol. 58, no. 4, pp. 412–417, 2009.

[122] S. Guo, C. zhang, W. Wang, T. Liu, and W. C. Tjiu "Preparation and characterization of polyurethane/multiwalled carbon nanotube composites," *Polym. Polym. Compos.*, vol. 16, no. 8, pp. 501–507, 2008.

[123] A. K. Barick and D. K. Tripathy, "Preparation and characterization of carbon nanofiber reinforced thermoplastic polyurethane nanocomposites," *J. Appl. Polym. Sci.*, vol. 124, no. 1, pp. 765–780, 2012.

[124] A. K. Barick and D. K. Tripathy, "Preparation, characterization and properties of acid functionalized multi-walled carbon nanotube reinforced thermoplastic polyurethane

nanocomposites," *Mater. Sci. Eng. B*, vol. 176, no. 18, pp. 1435–1447, 2011.

[125] E. Bilotti, R. Zhang, H. Deng, M. Baxendale, and T. Peijs, "Fabrication and property prediction of conductive and strain sensing TPU/CNT nanocomposite fibres," *J. Mater. Chem.*, vol. 20, no. 42, p. 9449, 2010.

[126] F. M. A.-O. S.M. Sapuan Y.A. El-Shekeil Fei-ling Pua, S. M. Sapuan, F. Pua, Y. a. El-Shekeil, and F. M. AL-Oqla, "Mechanical properties of soil buried kenaf fibre reinforced thermoplastic polyurethane composites," *Mater. Des.*, vol. 50, no. N/A, p. 467–470., 2013.

[127] L. Huang, N. Yi, Y. Wu, Y. Zhang, Q. Zhanf, Y. Huang, Y. Ma, and Y. Chen, "Multichannel and repeatable self-healing of mechanical enhanced graphene-thermoplastic polyurethane composites," *Adv. Mater.*, vol. 25, no. 15, pp. 2224–2228, 2013.

[128] K. A. Ames, "Elastomers for shoe applications," *Rubber Chem. Technol.*, vol. 77, no. 3, pp. 413–475, 2004.

[129] P. B. Maurus and C. C. Kaeding, "Bioabsorbable implant material review," *Operative Techniques in Sports Medicine*, vol. 12, no. 3. pp. 158–160, 2004

[130] C. Huang, R. Chen, Q. Ke, Y. Morsi, K. Zhang, and X. Mo, "Electrospun collagen-chitosan-TPU nanofibrous scaffolds for tissue engineered tubular grafts," *Colloids Surfaces B Biointerfaces*, vol. 82, no. 2, pp. 307–315, 2011.

[131] B. Hu Liu, M. Dong, W. Huang, J. Gao, K. Dai, J. Guo, S. and Z. G. G. Zheng, C. Liu, "Lightweight conductive graphene/thermoplastic polyurethane foams with ultrahigh compressibility for piezoresistive sensing," *J. Mater. Chem. C*, vol. 5, no. 1, pp. 73-83, 2017.

[132] S. K. Yeh, Y. C. Liu, W. Z. Wu, K. C. Chang, W. J. Guo, and S. F. Wang, "Thermoplastic polyurethane/clay nanocomposite foam made by batch foaming," *J. Cell. Plast.* , vol. 49, no. 2, pp. 119–130, 2013.

[133] H. A. Kharbas, T. Ellingham, M. Manitiu, G. Scholz, and L. S. Turng, "Effect of a cross-linking agent on the foamability of microcellular injection molded thermoplastic polyurethane," *J. Cell. Plast.*, vol. 53, no. 4, pp. 407-423, 2017.

[134] A. K. Nema, A. V. Deshmukh, K. Palanivelu, S. K. Sharma, and T. Malik, "Effect of exo- and endothermic blowing and wetting agents on morphology, density and hardness of thermoplastic polyurethanes foams," *J. Cell. Plast.*, vol. 44, no. 4, pp. 277–292, 2008.

[135] X. C. Wang, X. Jing, Y. Y. Peng, Z. K. Ma, X. T. Liu, L. S. Turng, and C. Y. Shen, "The effect of nanoclay on the crystallization behavior, microcellular structure, and mechanical properties of thermoplastic polyurethane nanocomposite foams," *Polym. Eng. Sci.*, vol. 56, no. 3, pp. 319–327, 2016.

[136] D. X. Yan, K. Dai, Z. D. Xiang, Z. M. Li, X. Ji, and W. Q. Zhang, "Electrical conductivity and major mechanical and thermal properties of carbon nanotube-filled polyurethane foams," *J. Appl. Polym. Sci.*, vol. 120, no. 5, pp. 3014–3019, 2011.

[137] J. Ling, W. Zhai, W. Feng, B. Shen, J. Zhang, and W. G. Zheng, "Facile preparation of lightweight microcellular polyetherimide/graphene composite foams for electromagnetic interference shielding," *ACS Appl. Mater. Interfaces*, vol. 5, no. 7, pp. 2677–2684, 2013.

[138] B. K. Kim, J. W. Seo, and H. M. Jeong, "Morphology and properties of waterborne

polyurethane/clay nanocomposites," *Eur. Polym. J.*, vol. 39, no. 1, pp. 85–91, 2003.

[139] J. Vega-Baudrit, M. Sibaja-Ballestero, P. Vázquez, R. Torregrosa-Maciá, and J. Miguel Martín-Martínez, "Properties of thermoplastic polyurethane adhesives containing nanosilicas with different specific surface area and silanol content," *Int. J. Adhes. Adhes.*, vol. 27, no. 6, pp. 469–479, 2007.

[140] P. H. Nam, P. Maiti, M. Okamoto, T. Kotaka, T. Nakayama, M. Takada, M. Ohshima, A. Usuki, N. Hasegawa, and H. Okamoto, "Foam processing and cellular structure of polypropylene/clay nanocomposites," *Polym. Eng. Sci.*, vol. 42, no. 9, pp. 1907–1918, 2002.

[141] D. X. Yan, K. Dai, Z. D. Xiang, Z. M. Li, X. Ji, and W. Q. Zhang, "Electrical conductivity and major mechanical and thermal properties of carbon nanotube-filled polyurethane foams," *J. Appl. Polym. Sci.*, vol. 120, no. 5, pp. 3014–3019, 2011.

[142] H. E. Naguib, C. B. Park, U. Panzer, and N. Reichelt, "Strategies for achieving ultra low-density polypropylene foams," *Polym. Eng. Sci.*, vol. 42, no. 7, pp. 1481–1492, 2002.

[143] S. N. Leung, A. Wong, L. C. Wang, and C. B. Park, "Mechanism of extensional stress-induced cell formation in polymeric foaming processes with the presence of nucleating agents," *J. Supercrit. Fluids*, vol. 63, no. N/A, pp. 187–198, 2012..

[144] M. H. Polley and B. B. S. T. Boonstra, "Carbon blacks for highly conductive rubber," *Rubber Chem. Technol.*, vol. 30, no. 1, pp. 170–179, 1957.

[145] A. Sircar, "Softer conductive rubber compounds by elastomer blending," *Rubber Chem. Technol.*, vol. 54, no. 4, pp. 820-834, 1981.

[146] E. M. Abdel-Bary, M. Amin, and H. H. Hassan, "Factors affecting electrical conductivity of carbon black-loaded rubber. I. Effect of milling conditions and thermal-oxidative aging on electrical conductivity of haf carbon black-loaded styrene–butadiene rubber," *J. Polym. Sci. Part A Polym. Chem.*, vol. 15, no. 1, pp. 197–201, 1971.